


RESEARCH ARTICLE



Persistent Acetylation of Histone H3 Lysine 56 Compromises the Activity of DNA Replication Origins

Roch Tremblay,^{a,b} Yosra Mehrjoo,^{a,b} Oumaima Ahmed,^{a,b} Antoine Simoneau,^{a,b} Mary E. McQuaid,^a El Bachir Affar,^{a,c} Corey Nislow,^d Guri Giaever,^d  Hugo Wurtele^{a,c}

^aMaisonneuve-Rosemont Hospital Research Center, Montreal, Québec, Canada

^bMolecular Biology Program, Université de Montréal, Montreal, Québec, Canada

^cDepartment of Medicine, Université de Montréal, Montreal, Québec, Canada

^dDepartment of Pharmaceutical Sciences, University of British Columbia, Vancouver, British Columbia, Canada

ABSTRACT In *Saccharomyces cerevisiae*, newly synthesized histones H3 are acetylated on lysine 56 (H3 K56ac) by the Rtt109 acetyltransferase prior to their deposition on nascent DNA behind replication forks. Two deacetylases of the sirtuin family, Hst3 and Hst4, remove H3 K56ac from chromatin after S phase. *hst3Δ hst4Δ* cells present constitutive H3 K56ac, which sensitizes cells to replicative stress via unclear mechanisms. A chemogenomic screen revealed that *DBF4* heterozygosity sensitizes cells to NAM-induced inhibition of sirtuins. *DBF4* and *CDC7* encode subunits of the Dbf4-dependent kinase (DDK), which activates origins of DNA replication during S phase. We show that (i) cells harboring the *dbf4-1* or *cdc7-4* hypomorphic alleles are sensitized to NAM, and that (ii) the sirtuins Sir2, Hst1, Hst3, and Hst4 promote DNA replication in *cdc7-4* cells. We further demonstrate that Rif1, an inhibitor of DDK-dependent activation of origins, causes DNA damage and replication defects in NAM-treated cells and *hst3Δ hst4Δ* mutants. *cdc7-4 hst3Δ hst4Δ* cells are shown to display delayed initiation of DNA replication, which is not due to intra-S checkpoint activation but requires Rtt109-dependent H3 K56ac. Our results suggest that constitutive H3 K56ac sensitizes cells to replicative stress in part by negatively influencing the activation of origins of DNA replication.

KEYWORDS DNA replication, chromatin structure, DNA damage response, *S. cerevisiae*, sirtuins, Hst3 and Hst4, histone H3 lysine 56 acetylation

INTRODUCTION

DNA replication initiates at multiple origins throughout chromosomes during the S phase of the cell cycle.¹ During G1, Cdt1 and Cdc6 load the MCM helicase complex on DNA at origins of replication bound by the origin recognition complex (ORC). Cyclin-dependent (CDK) and Dbf4-dependent (DDK) kinase activities promote the recruitment of factors including Cdc45 and the GINS complex to replication origins and activation of the MCM helicase during S phase. Melting of origin DNA resulting from MCM helicase activity allows the formation of two replication forks that travel in opposite directions along chromosomal DNA. Depending on the timing of their activation in S phase, eukaryotic origins are classified as early, mid, or late. Such sequential activation of origins has been shown to result at least in part from the recycling of limiting replication initiation factors from early to mid, and then to late replicating genomic regions.^{2,3} Such temporal organization of DNA replication is evolutionarily conserved among eukaryotes; however, the repertoire of cellular factors and molecular mechanisms modulating origin activation remains incompletely characterized.

© 2023 The Author(s). Published with license by Taylor & Francis Group, LLC. This is an Open Access article distributed under the terms of the Creative Commons Attribution-NonCommercial-NoDerivatives License (<http://creativecommons.org/licenses/by-nc-nd/4.0/>), which permits non-commercial re-use, distribution, and reproduction in any medium, provided the original work is properly cited, and is not altered, transformed, or built upon in any way. The terms on which this article has been published allow the posting of the Accepted Manuscript in a repository by the author(s) or with their consent.

Supplemental data for this article can be accessed online at <https://doi.org/10.1080/10985549.2023.2259739>

Address correspondence to Hugo Wurtele, hugo.wurtele@umontreal.ca.

Received 21 October 2022

Revised 8 August 2023

Accepted 9 August 2023

Replication fork progression can be halted upon encountering DNA lesions induced by various environmental or endogenous genotoxins.⁴ This engenders a state of replicative stress which can prevent completion of chromosomal duplication, thereby causing genomic instability. Stalled replication forks activate Mec1 (ATR in humans), the apical kinase of the intra-S phase checkpoint response in yeast.⁴ In turn, Mec1 promotes activation of the kinase Rad53 via one of two pathways that depend upon either the replication fork component Mrc1 or the adaptor protein Rad9.⁵ Activated Mec1 and Rad53 phosphorylate a plethora of substrates to (i) promote the stability of stalled replication forks, and (ii) to prevent further activation of replication origins.⁶ In yeast, this latter effect has been shown to depend on Rad53-dependent phosphorylation of the key replication factors Dbf4 and Sld3, which prevents activation of MCM helicase complexes at origins that have not yet been fired.⁷ Intra-S phase checkpoint-dependent inhibition of origin activity is important to prevent inordinate accumulation and eventual collapse of stalled replication forks during periods of genotoxic stress.⁸

Histone posttranslational modifications are critical determinants of DNA replication dynamics and origin activity.^{9,10} Among those modifications, histone lysine acetylation can either promote and inhibit origin activity depending on the identity of the modified residue and/or chromosomal context.¹¹ The sirtuin family of histone deacetylases is well-conserved throughout evolution, and several of its members have been shown to influence DNA replication and repair.¹² The yeast *Saccharomyces cerevisiae* possesses five sirtuins: the founding member, Sir2, and homologues of Sir Two 1–4 (Hst1–4).¹² Sir2 targets histone H4 lysine 16 acetylation (H4 K16ac), which regulates origins at the rDNA locus and telomeres.^{13,14} Hst1 forms a complex with Sum1 and Rfm1 and modulates the activity and chromatin structure of a subset of origins genome-wide.^{15,16} While the impact of Hst2 on DNA replication has not been directly assessed, at least some of the functions of this sirtuin are known to be partially redundant with those of Sir2, as overexpressed Hst2 rescues gene silencing defects caused by *sir2Δ*.^{17,18}

The only known histone substrate of the redundant sirtuins Hst3 and Hst4 is acetylated H3 lysine 56 (H3 K56ac).¹⁹ This modification is catalyzed by the acetyltransferase Rtt109 on newly synthesized histones H3 prior to their deposition onto nascent DNA during S phase.^{20,21} After S phase, Hst3 and Hst4 remove H3 K56ac chromosome-wide such that a large majority of nucleosomes do not harbor H3 K56ac at the start of the next cell cycle. While under normal circumstances the bulk of H3 K56ac is removed by Hst3 during G2, Hst4 can compensate for its absence. As such, the stoichiometry of H3 K56ac approaches 100% throughout the cell cycle in *hst3Δ hst4Δ* double mutants.^{19,22} While constitutive H3 K56ac has been shown to cause spontaneous DNA damage, thermosensitivity, and increased sensitivity to genotoxins that cause replicative stress,^{19,23,24} the molecular mechanisms underlying such striking phenotypes remain poorly understood.

Nicotinamide (NAM) is a noncompetitive pan-inhibitor of sirtuins.²⁵ Our group previously performed genetic screens in *S. cerevisiae* with the goal of identifying genes whose homozygous deletion (i.e. complete loss-of-function) confers either fitness defect or advantage in response to NAM-induced sirtuin inhibition and consequent H3 K56 hyperacetylation.²⁶ These screens revealed that several genes encoding regulators of the DNA replication stress response promote resistance to NAM-induced elevation in H3 K56ac caused by inhibition of Hst3 and Hst4.^{26,27} Previously published data also indicate that cells lacking HST3 are defective in the maintenance of artificial chromosomes harboring a reduced number of DNA replication origins,²⁸ further linking H3 K56ac with the regulation of DNA replication dynamics. Here, we present the results of a genome-wide screen aimed at identifying genes whose haploinsufficiency modulates cell fitness in response to NAM. Overall, we found that (i) appropriate dosage of genes involved in various cellular pathways influence cell fitness in response to NAM, (ii) factors promoting DNA replication origin activation are critical for survival in the absence of Hst3 and Hst4 activity, and (iii) abnormal persistence of the acetylation of new

histones H3 on lysine 56 throughout the cell cycle compromises the activity of replication origins.

RESULTS

A genetic screen to identify genes modulating cellular fitness in response to NAM. We performed a screen using the pooled yeast strains of the heterozygote diploid collection to identify haploinsufficient genes that influence cell fitness upon NAM exposure (Supplementary material, Table S1). Using a Z-score cut-off of ± 2.58 (99% cumulative percentage), the screen identified 131 and 58 genes whose heterozygosity caused reduced or increased fitness, respectively, during propagation for 20 generations in YPD medium containing 41 mM NAM (Fig. 1A). This list of genes presents only modest overlap with that obtained from our previously published screen using the homozygote deletion strain collection (Fig. 1B), suggesting that most of the genes identified in the latter screen are not haploinsufficient with regard to NAM sensitivity. We note that such limited overlap between screens performed on the homozygous and heterozygous deletion collections has also been observed in several other chemogenetic screens.²⁹ Gene ontology (GO) term analysis of genes whose heterozygosity sensitizes cells to NAM revealed an obvious enrichment in DNA replication and DNA

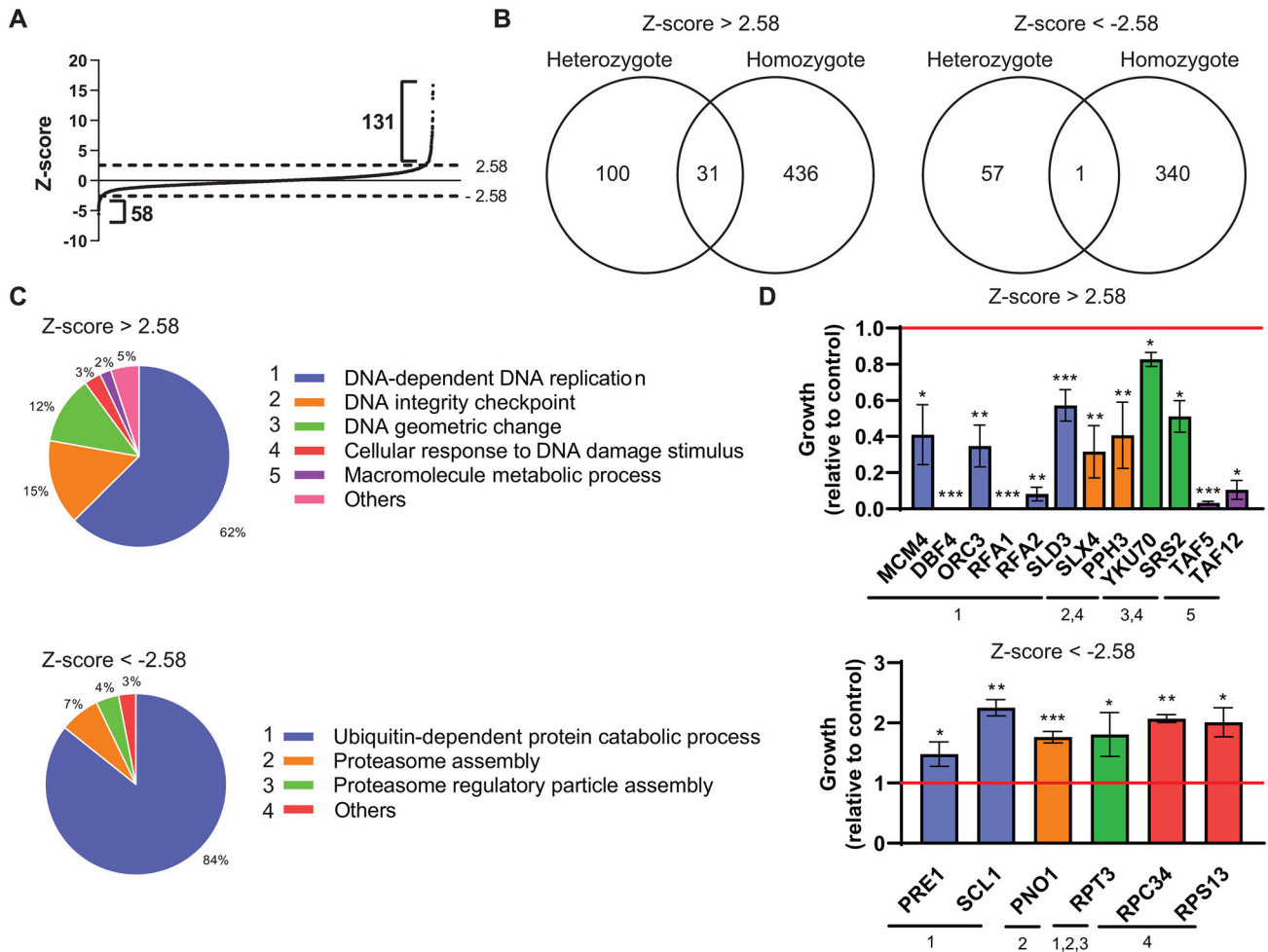


FIG 1 A chemogenomic screen identifies genes whose heterozygosity modulates cell fitness upon NAM exposure. (A) Z-score of individual heterozygote diploid yeast strains after 20 generations in a medium containing 41 mM NAM. GO-terms of genes for which the Z-scores is > 2.58 or < -2.58 were further analyzed in B and C. (B) Venn diagram comparing the heterozygote diploid screen presented here with a previous one performed with homozygote diploid deletion strains.²⁶ (C) GO-terms associated with genes presenting Z-scores > 2.58 or < -2.58 . (D) Growth competition assays for selected heterozygote deletion strains presenting Z-scores > 2.58 or < -2.58 . WT and mutant cells were mixed 1:1 and grown in YPD \pm 41 mM NAM for 20 generations. The fraction of mutant/WT cells in the culture was assessed by plating on appropriate selective media followed by colony counting. Colors and numbers below strain names refer to the GO-terms highlighted in C.

damage response pathway, whereas terms reflecting proteasome-related and catabolic processes were associated with mutations that enhanced fitness in NAM (Fig. 1C and Table 1 and Table 2).

We next sought to validate individual heterozygous mutations representing the main categories of “hits” identified in the screen. WT diploid and heterozygote mutant strains of interest (*yfg1Δ::KanMX/YFG1*) were mixed in a 1:1 ratio and incubated for 20 generations in YPD ± NAM. Appropriate dilutions of cells were then plated on YPD-agar ± G418, and the ratio of the number of heterozygous mutant (G418-resistant) vs WT (G418-sensitive) colonies was calculated (Fig. 1D). These competition assays confirmed the expected impact of heterozygous mutations causing diminished cell fitness in NAM-containing medium, thereby validating our screen results. While significant improvement in growth was observed for individual heterozygous mutants expected to promote fitness in NAM, we note that heterozygous mutations causing improved fitness in response to NAM displayed generally lower absolute Z-scores than those reducing fitness (Fig. 1A, Supplementary material, Table S1).

Reduced activity of DNA replication origins sensitizes cells to NAM. As mentioned previously, cells lacking Hst3 have been shown to present defects in the maintenance of an artificial chromosome harboring reduced number of DNA replication origins, revealing a potential link between this sirtuin and origin activity.²⁸ Nevertheless, the mechanistic basis of the effect of Hst3 on origins remains unclear. Remarkably, 6 of the 11 essential DNA replication genes identified in the screen as promoting NAM resistance are members of the prereplicative complex (ORC3 and MCM4) or involved in various steps of origin activation (DBF4, SLD2, SLD3, PSF2). We therefore decided to further investigate the possible relationship between NAM sensitivity and origin activity. We focused our efforts on the Dbf4-dependent kinase (DDK), a complex formed by Dbf4 and the Cdc7 kinase which phosphorylates subunits of the MCM replicative helicase to permit its activation during S phase.³⁰ Even though *CDC7* was not identified as being haploinsufficient with regards to NAM resistance in our screen, haploid cells expressing hypomorphic temperature sensitive alleles of either *DBF4* (*dbf4-1*) or *CDC7* (*cdc7-4*) were found to be NAM-sensitive at semipermissive temperatures (Fig. 2A to C). We note that the abundance of Dbf4 has been reported to be limiting for DDK activity during S phase;³ this might explain why heterozygosity of *DBF4*, but not *CDC7*, caused NAM sensitivity in the context of our screen. Interestingly, we also found that *bob1-1 cdc7Δ* cells, which harbor a mutation in *MCM5* that bypasses DDK-dependent phosphorylation of the MCM complex that is necessary for origin activation,³¹ are not sensitive to NAM (Fig. 2C and D). This argues that the MCM complex is likely to be the relevant target of DDK in this context, and suggests that impaired activation of replication origins sensitizes cells to NAM.

We next evaluated S phase progression in NAM-treated *cdc7-4* and *dbf4-1* cells (Fig. 2E and F). After alpha factor arrest in G1, cells were released toward S phase for 30 min at the permissive temperature of 25 °C. NAM was then added to the medium and cells were rearrested at the subsequent G1/S border by incubation at the nonpermissive temperature of 37 °C, before being released in the second S phase at a semipermissive temperature (32 °C for *dbf4-1* and 30 °C for *cdc7-4*). The results indicate that NAM exposure during one cell cycle noticeably delays S phase completion in *cdc7-4* and *dbf4-1* mutants, consistent with a negative effect of NAM on DNA replication dynamics in these cells.

Rap1-interacting factor 1 (Rif1) acts in complex with the phosphatase Glc7 to reverse DDK-dependent MCM phosphorylation, thereby inhibiting origin activation.^{32–35} Moreover, a previous screen performed by our group identified *RIF1* among the few yeast genes whose homozygous deletion improved cell fitness in NAM-containing medium.²⁶ We found that *RIF1* deletion rescued NAM-induced growth defects of *cdc7-4* cells at the semipermissive temperature (Fig. 3A). Moreover, N-terminal truncation or mutations in the Glc7-interacting motif (*rif1*-RVxF/SILK) of Rif1, both of which were previously shown to partially suppress the temperature sensitivity of *cdc7-4* mutants by

TABLE 1 GO term analysis of gene with positive Z-score in NAM fitness assay

Gene Ontology term	Cluster frequency	Genome frequency	Corrected P-value	FDR	False Positives	Genes annotated to the term
Macromolecule metabolic process	98 of 131 genes, 74.8%	3217 of 7166 genes, 44.9%	1.76e-09	0.00%	0.00	PSY2, PPH3, RFA2, BSD2, MAK10, GFD1, YKU80, MRC1, ALG2, PRP9, TAF10, SMT3, RRP4, KRE29, DBF2, RPN13, UTP15, NPP1, RPL32, PKC1, YKU70, MTR3, MNL1, TIF11, SMX2, GSP1, HYP2, TFC1, CUS1, PSF2, CFT1, SLD2, TAF5, TAF6, PIN4, RRP45, WRS1, SPN1, MPS3, SLD3, PDC2, UBP3, ERD1, TOF1, SGT2, SRB7, PUT3, UFD4, PRI2, YHC1, ACA1, POL32, TIF2, NOP58, TFB1, ASC1, MED11, MCM4, LSM2, DBF4, MCD4, GLC7, FPR3, NUP145, TAF7, RRP42, RFA1, SSL2, SRS2, BRE5, NMD4, SEN1, DBP2, KAP95, KKQ8, STE11, DUN1, SLX4, CDC12, TAF8, NIP1, MAK31, UBC9, NET1, DPB3, KEX2, NUP82, SSN3, TIP41, LAS1, DPB4, ORC3, SPT15, UBP8, BDP1, SUI1, SAS10, TAF12
DNA-dependent DNA replication	18 of 131 genes, 13.7%	133 of 7166 genes, 1.9%	1.78e-08	0.00%	0.00	DPB3, SLD2, MCM4, DBF4, MRC1, POL32, PSF2, PRI2, RFA2, DUN1, SLX4, TOF1, SEN1, RFA1, SLD3, GLC7, ORC3, DPB4
Cellular response to DNA damage stimulus	27 of 131 genes, 20.6%	357 of 7166 genes, 5.0%	1.37e-07	0.00%	0.00	PSY2, PPH3, RFA2, DUN1, SLX4, IRC21, PRI2, YKU80, PSF2, POL32, MRC1, TFB1, SLD2, DPB3, MCM4, KRE29, GLC7, NUP145, DPB4, PIN4, RFA1, SLD3, SSL2, SRS2, SEN1, TOF1, YKU70
DNA integrity checkpoint	10 of 131 genes, 7.6%	55 of 7166 genes, 0.8%	3.53e-05	0.00%	0.00	PIN4, PPH3, PSY2, DUN1, GLC7, SLX4, SLD2, TOF1, DBF4, MRC1
DNA geometric change	11 of 131 genes, 8.4%	71 of 7166 genes, 1.0%	4.14e-05	0.00%	0.00	MCM4, YKU70, SLD2, SRS2, SEN1, YKU80, PSF2, RFA1, SSL2, SLD3, RFA2
Biological regulation	66 of 131 genes, 50.4%	2096 of 7166 genes, 29.2%	0.00019	0.00%	0.00	DFR1, GSP1, HYP2, SLD2, TAF6, PIN4, RRP45, SPN1, MPS3, PDC2, UBP3, ERD1, TOF1, SRB7, SGT2, PUT3, PSY2, PPH3, RFA2, BSD2, YKU80, MRC1, RRP4, DBF2, ZRC1, RPN13, UTP15, PKC1, MTR3, YKU70, KAP95, KKQ8, STE11, DUN1, SLX4, CDC12, NET1, DPB3, SSN3, TIP41, DPB4, ORC3, SPT15, BDP1, SUI1, UFD4, ECM25, YHC1, ACA1, TFB1, MED11, ASC1, DBF4, FPR3, GLC7, NUP145, TAF7, RRP42, RFA1, SSL2, SRS2, BRE5, SEN1, NMD4, FTH1, DBP2
Cellular component organization or biogenesis	73 of 131 genes, 55.7%	2453 of 7166 genes, 34.2%	0.00024	0.00%	0.00	SPT15, ATP11, LAS1, DPB4, ORC3, TIM10, SAS10, TAF12, SUI1, BDP1, UBP8, CDC12, SLX4, KAP95, NUP82, DPB3, UBC9, NET1, NIP1, TAF8, RFA1, SSL2, RRP42, GLC7, FPR3, TAF7, NUP145, MCD4, DBP2, SRS2, SEN1, ECM25, YHC1, UFD4, VTC3, MED11, MCM4, LSM2, DBF4, CDC3, NOP58, SPN1, MPS3, SLD3, RRP45, PUT3, TOF1, HYP2, TFC1, GSP1, TIF11, SMX2, TAF6, TAF5, SLD2, PSF2, CUS1, DBF2, TAF10, RRP4, TIM12, YJL160C, PKC1, YKU70, MTR3, UTP15, RFA2, ECM30, PPH3, PSY2, PRP9, YKU80, MRC1
Cellular process	117 of 131 genes, 89.3%	5175 of 7166 genes, 72.2%	0.00113	0.00%	0.00	TIF11, MNL1, DFR1, SMX2, GSP1, TFC1, HYP2, PSF2, CUS1, CFT1, SLD2, TAF5, TAF6, DPP1, NKP1, PIN4, CAR2, WRS1, RRP45, SPN1, MPS3, SLD3, UBP3, PDC2, ERD1, TOF1, SGT2, SRB7, PUT3, PPH3, PSY2, RFA2, ECM30, BSD2, IRC21, MAK10, YKU80, MRC1, ALG2, PRP9, SMT3, TAF10, RRP4, KRE29, DBF2, ZRC1, HOM6, RPN13, UTP15, RPL32, NPP1, CCT3, YJL160C, TIM12, PKC1, YKU70, MTR3, CCT6, KKQ8, KAP95, STE11, DUN1, SLX4, SAM2, CDC12, TAF8, NIP1, MAK31, UBC9, NET1, DPB3, SSN3, TIM10, TIP41, LAS1, ORC3, DPB4, SPT15, ATP11, DOG1, BDP1, UBP8, SUI1, SAS10, TAF12, UFD4, VTC3, ECM25, PRI2, YHC1, ACA1, POL32, MIS1, NOP58, TIF2, CDC3, TFB1, ASC1, MED11, MCM4, LSM2, DBF4, MCD4, GLC7, FPR3, TAF7, NUP145, RRP42, RFA1, TCP1, SSL2, BRE5, SRS2, SEN1, NMD4, CCT2, DBP2

TABLE 2 GO term analysis of genes with negative Z-score in NAM fitness assay

Gene Ontology term	Cluster frequency	Genome frequency	Corrected P value	FDR	False Positives	Genes annotated to the term
Ubiquitin-dependent protein catabolic process	18 of 58 genes, 31.0%	226 of 7166 genes, 3.2%	2.46e-11	0.00%	0.00	RPT2, TRE2, SSE1, SCL1, PRE7, PRE8, RPT3, RPN5, RPN11, MET30, PRE3, RPT1, RPN12, PRE1, PUP2, PRE6, RPT5, RPN6
Proteasome assembly	7 of 58 genes, 12.1%	35 of 7166 genes, 0.5%	3.04e-06	0.00%	0.00	RPT1, RPN6, RPN11, RPT5, PNO1, RPT2, RPT3
Proteasome regulatory particle assembly	4 of 58 genes, 6.9%	11 of 7166 genes, 0.2%	0.00042	0.00%	0.00	RPT1, RPT2, RPT3, RPT5
Catabolic process	21 of 58 genes, 36.2%	936 of 7166 genes, 13.1%	0.00211	0.00%	0.00	RPT2, TRE2, SSE1, SCL1, PRE7, PRE8, RPT3, RPN5, LSM7, RPN11, MET30, RPL13B, CDC39, RPN12, RPT1, PRE3, PRE1, PRE6, PUP2, RPT5, RPN6

eliminating Rif1 binding to Glc7,^{33,36} also suppressed the NAM sensitivity of *cdc7-4* cells (Fig. 3A). Overall, these data suggest that Rif1/Glc7-dependent dephosphorylation of MCM influences NAM sensitivity.

We and others previously showed that NAM treatment causes replicative stress and DNA damage in yeast.^{19,26,27} Since lack of MCM phosphorylation by DDK causes sensitivity to replicative stress-inducing drugs,^{37,38} we tested the impact of *RIF1* deletion on NAM-induced DNA damage. Compared to WT, *rif1Δ* cells presented reduced NAM-induced histone H2A S129 phosphorylation (Fig. 3B) and Rad52-YFP foci formation (Fig. 3C), two markers of replicative stress-induced DNA damage.^{39,40} Importantly, lack of Rif1 did not compromise the formation of ionizing radiation (IR)-induced Rad52 foci, which are not primarily caused by replication-associated DNA lesions. Interestingly, NAM-induced accumulation of cells in S phase was also rescued by deletion of *RIF1* (Fig. 3D). We note that, in addition to its role in regulating DNA replication, Rif1 is known to limit telomere length by inhibiting telomerase activity.⁴¹ Moreover we previously showed that cells with short telomeres are sensitive to NAM-induced sirtuin inhibition²⁷; we therefore considered the possibility that abnormal telomere elongation in *rif1Δ* cells might favor NAM resistance. Contrary to this notion, deletion of *RIF1* suppressed NAM-induced growth and S phase progression defects in telomerase-defective *est2Δ* cells (Fig. 3D and E), indicating that the role of Rif1 in modulating NAM sensitivity is independent of its influence on telomerase activity.

Several sirtuins act to promote DNA replication in *cdc7-4* cells. We next evaluated the contribution of individual sirtuins to the NAM sensitivity of *cdc7-4* cells. Our data indicate that deletion of *SIR2* or *HST1*, but not *HST2*, causes synthetic temperature sensitivity when combined with *cdc7-4* (Fig. 4A). As mentioned previously, both Sir2 and Hst1 are known to modulate DNA initiation at distinct subsets of origins of replication.^{11,13–16} Consistently, deletion of *SIR2* or *HST1* delayed progression through S phase in *cdc7-4* cells at the semipermissive temperature of 30 °C (Fig. 4B). We also found that deletion of both *HST3* and *HST4*, but not of either gene alone, increased the temperature sensitivity of *cdc7-4* (Fig. 4C), in accord with the known functional redundancy of Hst3/Hst4 with respect to deacetylation of histone H3 lysine 56, the only known chromatin substrate of these enzymes.^{19,22}

Since the possible impact of H3 K56ac on DNA replication dynamics is poorly understood,²⁸ we sought to further characterize the role of Hst3/4 in modulating the phenotypes of *cdc7-4* cells. We first evaluated whether H3 K56ac is responsible for the S phase delay observed in *cdc7-4* upon NAM treatment. After alpha factor-mediated G1 arrest, we released *cdc7-4* or *cdc7-4 rtt109Δ* cells in the cell cycle in the presence or absence of NAM at a permissive temperature (25 °C) to allow cells to reach G2/M. Cells were then arrested at the subsequent G1/S transition by incubation at the

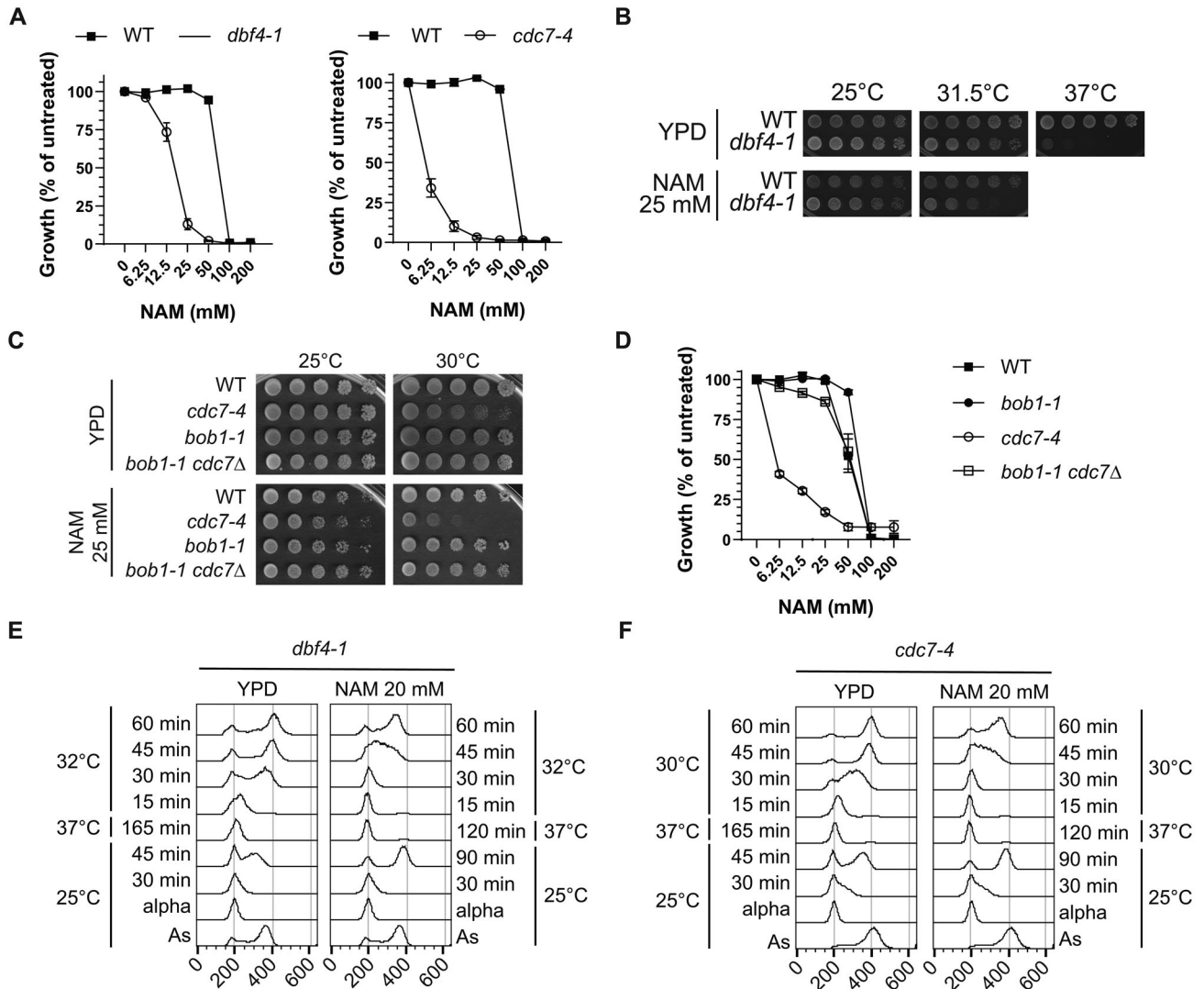


FIG 2 Yeast cells harboring hypomorphic alleles of *CDC7* or *DBF4* are sensitive to NAM. (A) Haploid WT, *dbf4-1* and *cdc7-4* cells were incubated at the semipermissive temperature of 30°C in medium containing the indicated concentration of NAM. OD₆₃₀ readings were taken at 72 h to quantify cell proliferation (see Materials and Methods). (B) Five-fold serial dilutions of cell cultures were spotted on YPD-agar and YPD-agar + 25 mM NAM plates and incubated at the indicated temperature. (C) As in B. (D) Cells were treated as in A. (E) *dbf4-1* cells were arrested in G1 using alpha factor (alpha) and released toward S at 25°C. After 30 min, 20 mM NAM was added or not to the culture. Cells were further incubated for 15 min (without NAM) or 60 min (with NAM) before incubation at the restrictive temperature of 37°C for the indicated time to block cells in early S phase. Cells were then incubated at the semirestrictive temperature of 32°C. Samples were taken for DNA content analysis by flow cytometry at the indicated time points. As, asynchronous. Cell cycle profiles before NAM treatment are duplicated to improve visualization of cell cycle progression. (F) *cdc7-4* cells were treated as in E except that after the arrest in early S at 37°C, cells were transferred at a semirestrictive temperature of 30°C.

nonpermissive temperature of 37°C, followed by release toward S phase at the semi-permissive temperature of 30°C. The data indicate that defects in S phase progression induced by incubation in NAM during one cell cycle are independent of *RTT109* (Fig. 4D), and therefore do not require H3 K56ac since *rtt109Δ* abolishes this modification.⁴² This suggests that H3 K56ac accumulation during a single cell cycle, i.e., to a stoichiometry of no more than 50%, is insufficient to cause S phase progression defects in *cdc7-4* cells. It is therefore plausible that NAM-induced S phase delays are due to inhibition of sirtuins other than Hst3/4 in these conditions.

To further validate these observations, we tested whether accumulation of H3 K56ac during G2/M influences S phase progression in the subsequent S phase (Fig. 4E and F). *cdc7-4* cells were arrested in G1 using alpha factor and then released toward S phase at the permissive temperature of 25°C in nocodazole-containing medium to prevent mitosis. After 30 min, NAM was added or not and cells were further incubated

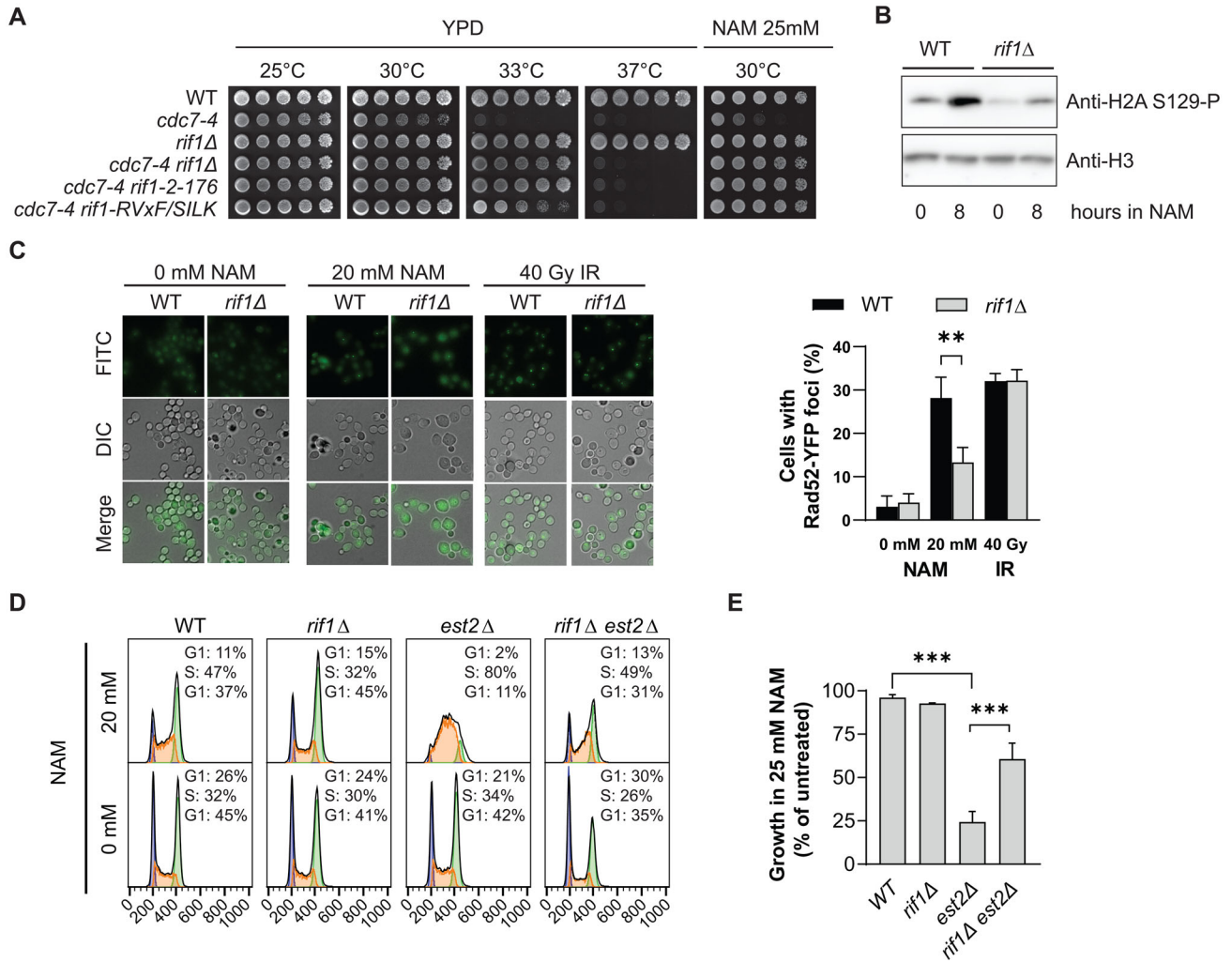


FIG 3 *RIF1*-dependent inhibition of origin activity impairs cell viability in NAM. (A) Five-fold serial dilutions of cell cultures were spotted on YPD-agar and YPD-agar + 25 mM NAM plates and incubated at the indicated temperature. (B) WT and *rif1Δ* cells were exposed to 20 mM NAM for 8 h at 30 °C and total cell extracts were processed for immunoblotting. (C) Exponentially growing WT and *rif1Δ* cells in SC medium were treated with 20 mM NAM for 8 h at 30 °C, or exposed to 40 Gy of ionizing radiations followed by incubation for 1 h at 30 °C. Samples were then processed for fluorescence microscopy. Left panel: representative microscopy images. Right panel: quantification of cells containing Rad52-YFP foci. Graph bars represent mean ± SEM of three independent experiments. ***P* < 0.01, unpaired two-tailed Student's *t* test. (D) Exponentially growing cells were incubated at 25 °C in YPD containing 20 mM NAM for 8 h. Samples were taken for flow cytometry analysis of DNA content. Blue, orange, and green regions represent G1, S, and G2/M cell populations, respectively. (E) The ratio of OD₆₃₀ readings of cells treated with 25 mM NAM vs nontreated after 48 h of growth in 96-well plates is presented. Graph bars represent mean ± SEM of three independent experiments each containing four technical replicates. ***FDR-adjusted *P*-value < 0.001, values were calculated using unpaired multiple *t* test and FDR analysis (Benjamini, Krieger, and Yekutieli method).

until they reached G2/M (60 min). Immunoblot analysis indicates that at that point NAM treatment elevated H3 K56ac as a result of Hst3/4 inhibition. Cells were then released from nocodazole in a medium containing NAM or not at the nonpermissive temperature of 37 °C for 75 min so that they would accumulate at the next G1/S border. Immunoblot analysis demonstrates that the absence of NAM in the medium allows Hst3/4 to deacetylate H3 K56ac during that time period. Finally, cells were released at the semipermissive temperature of 30 °C into S phase. The results clearly indicate that transient increase of H3 K56ac during G2/M does not compromise the subsequent S phase (compare subpanels E, I, L in Fig. 4F). Importantly, while Hst3 and Hst4 both deacetylate H3 K56ac, their expression is differently regulated during the cell cycle; Hst3 is expressed predominantly in G2 whereas Hst4 levels peak in late mitosis and G1.²² The above data are therefore consistent with the fact that deletion of both *HST3* and *HST4*, leading to constitutive H3 K56ac, is necessary to observe

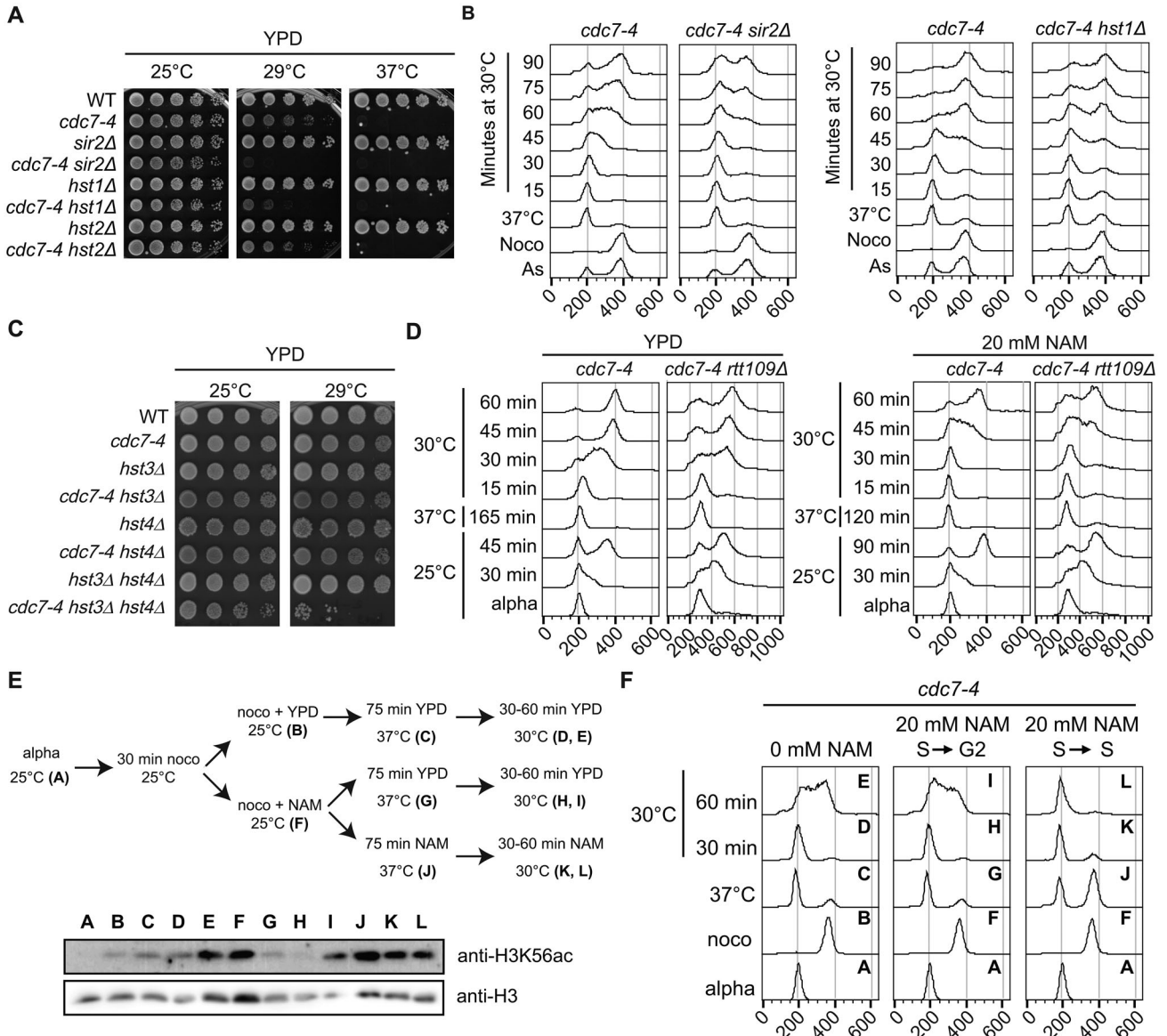


FIG 4 Several sirtuins act to promote DNA replication in *cdc7-4* cells. (A) Five-fold serial dilutions of cell cultures were spotted on solid YPD medium and incubated at the indicated temperature. (B) Asynchronously growing cells were arrested in mitosis using nocodazole (noco). Arrested cells were washed and incubated at 37°C for 2 h to synchronize them at the G1/S border. Cells were then incubated at 30°C. Samples were taken for DNA content analysis by flow cytometry at the indicated time points. As, asynchronous. (C) Cells were treated as in A. (D) *cdc7-4* or *cdc7-4 rtt109Δ* cells were arrested in G1 using alpha factor (alpha) and released toward S at 25°C. After 30 min, 20 mM NAM was added to half of the culture. Cells were incubated for 15 min (cells without NAM) or 60 min (cells with NAM) before being transferred to 37°C for the indicated time to block cells at the next G1/S border. Cells were then incubated at a semirestrictive temperature of 30°C. Samples were taken for DNA content analysis by flow cytometry at the indicated time points. Cell cycle profiles of samples taken before NAM treatment are duplicated to facilitate visualization of cell cycle progression. (E–F) Schematic representation of the experiment. Letters represent different time points. *cdc7-4* cells were arrested in G1 using alpha factor (alpha) and released toward S in the presence of nocodazole (noco) for 30 min at 25°C. Then, 20 mM of NAM was added to half of the culture. Cells were incubated at 25°C for 60 min. Nocodazole-arrested cells were then washed. Cells not treated with NAM were resuspended in YPD medium. Cells treated with NAM were resuspended either in YPD or YPD containing 20 mM NAM. Then, cells from all three conditions were incubated at 30°C. Samples were collected for (E) immunoblotting or for (F) DNA content analysis by flow cytometry.

synthetic temperature sensitivity with *cdc7-4*, i.e., *hst3Δ cdc7-4* are not more temperature sensitive than *cdc7-4* cells (Fig. 4C).

A fraction of the cells that were arrested in G1, released toward the cell cycle in nicotinamide and nocodazole, and then released from nocodazole at 37°C in the presence of nicotinamide, appears to be delayed in completing mitosis (Fig. 4F panel J). However, we note that (i) a significant fraction of cells reaches the G1/S border in these conditions (Fig. 4F panel J), and that (ii) all of them reach the G1/S border, but do not

progress into S phase upon further incubation at 30 °C (Fig. 4F panel K). This suggests that the incapacity of cells exposed to nicotinamide throughout S, G2/M, and the subsequent G1, to progress through S phase is unlikely to merely be the result of an extended G2/M duration. In turn, this supports our initial conclusion that transient, as opposed to sustained, exposure to nicotinamide only during S and subsequent G2/M is insufficient to delay the progression of the next S phase.

While the precise mechanism responsible for the G2/M delay observed when nicotinamide exposure is maintained during release of *cdc7-4* cells from nocodazole at 37 °C is unclear, several possibilities exist. First, treatment of cells with nicotinamide, or deletion of *HST3* and *HST4*, cause defective sister chromatid cohesion in cells treated with nocodazole.⁴³ Moreover, Cdc7 and Dbf4 are involved in sister chromatid cohesion and chromosome segregation.^{44,45} The above considerations raise the possibility that sustained nicotinamide-induced cohesion defects may activate the mitotic spindle checkpoint⁴⁶ and consequently delay mitosis in *cdc7-4* cells released from nocodazole at the restrictive temperature. In contrast, sustained exposure to nicotinamide during S and subsequent G2/M phases mimics *HST3* deletion with regards to H3 K56ac accumulation.¹⁹ Cells lacking Hst3 (i) spontaneously accumulate foci of the homologous recombination (HR) protein Rad52,⁴⁷ and (ii) are defective in HR-dependent sister chromatid exchanges.⁴⁸ It is therefore also possible that sustained nicotinamide-induced inhibition of Hst3 in cells released from nocodazole might activate the DNA damage checkpoint response, thereby also contributing to the observed mitotic delays.

Lack of Hst3/Hst4 activity compromises S phase progression in *cdc7-4* cells. We next investigated the mechanistic basis of the synthetic phenotypes of *cdc7-4 hst3Δ hst4Δ* cells. We found that lack of *RIF1* rescued the synthetic temperature sensitivity of *cdc7-4 hst3Δ hst4Δ* cells (Fig. 5A), suggesting that Cdc7-dependent activation of origins of replication promotes survival in *hst3Δ hst4Δ* mutants. Strikingly, we also found that *cdc7-4 hst3Δ hst4Δ* cells displayed strong RIF1-dependent inhibition of S phase progression when released from alpha factor-mediated G1 arrest toward S at 30 °C compared to either *hst3Δ hst4Δ* or *cdc7-4* (Fig. 5B). Such S phase progression defect was not observed at the permissive temperature of 25 °C, indicating that the impact of reduced Cdc7 activity (due to incubation at the semipermissive temperature of 30 °C for *cdc7-4*) on DNA replication is strongly exacerbated by deletion of *HST3* and *HST4* (Fig. 5C). This phenotype was rescued by expression of plasmid-borne copy of *HST3* (Fig. 5D), consistent with the notion that lack of both *HST3* and *HST4* is necessary to observe synthetic phenotypes with *cdc7-4*. The observed DNA replication defect does not appear to result from compromised release from alpha factor-mediated G1 arrest, since asynchronously growing *cdc7-4 hst3Δ hst4Δ* cells also accumulate in early S when incubated at 30 °C (Fig. 5E). Moreover, the budding index of *cdc7-4 hst3Δ hst4Δ* cells released from alpha factor-mediated G1 block toward S phase at 30 °C was comparable to that of *cdc7-4* cells (\approx 50-60% of cells with detectable buds; Fig. 5F) even though the former cells present barely detectable S phase progression in these conditions (Fig. 5B). We note that the small size of buds at 45 and 60 min postrelease from alpha factor rendered precise assessment of budding index challenging. To further confirm our results, we performed an experiment in which *cdc7-4* and *cdc7-4 hst3Δ hst4Δ* cells were released from alpha factor-induced G1 arrest toward S at the nonpermissive temperature of 39 °C for 3 h, thereby allowing time for buds to become larger while preventing Cdc7 activity and, consequently, initiation of DNA synthesis at origins (Fig. 5G). After monitoring the budding index, the temperature of the culture was decreased to 30 °C for 30 min to evaluate S phase progression (Fig. 5G). While for unknown reasons the fraction of *cdc7-4 hst3Δ hst4Δ* and *cdc7-4* mutants with detectable buds did not reach more than 60 to 80%, respectively, in these conditions (Fig. 5H), S phase progression remained completely blocked in *cdc7-4 hst3Δ hst4Δ*, but not *cdc7-4* cells, after incubation at 30 °C (Fig. 5G). Overall, the data indicate that even though *cdc7-4 hst3Δ hst4Δ* cells enter S phase at the semipermissive temperature of 30 °C, DNA replication progression is strongly inhibited in a RIF1-dependent manner in these conditions.

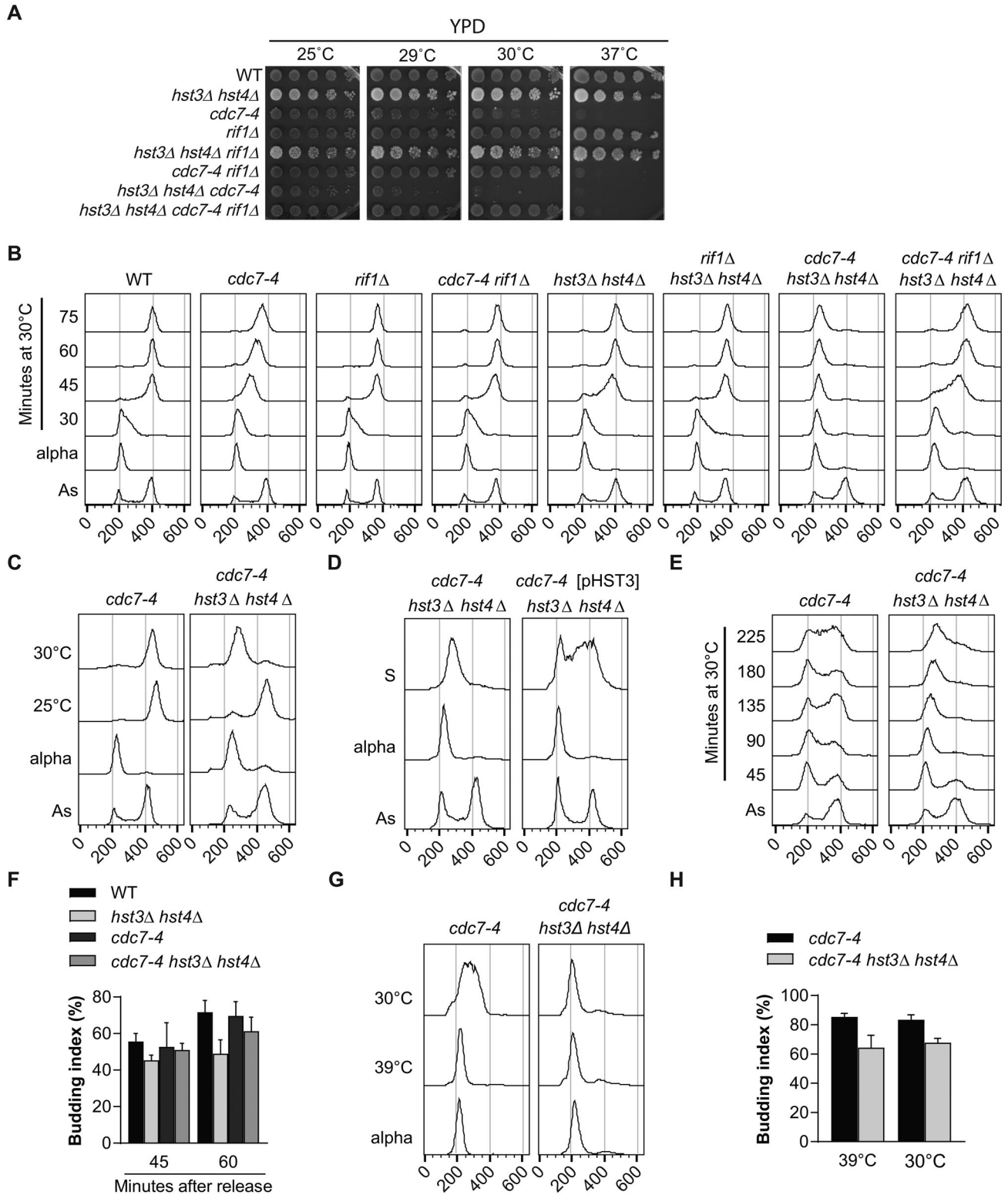


FIG 5 Deletion of *HST3* and *HST4* inhibits *S* phase progression in *cdc7-4* cells. (A) Five-fold serial dilutions of cell cultures were spotted on solid YPD medium and incubated at the indicated temperature. (B) Cells were arrested in G1 using alpha factor at 25 °C (alpha) and released toward *S* phase at 30 °C. Samples were taken for DNA content analysis by flow cytometry at the indicated time points. As, asynchronous. (C) Cells were arrested in G1 using alpha factor at 25 °C (alpha) and released toward *S* phase at 25 °C or 30 °C for 90 min before harvest. Samples were taken for DNA content analysis by flow cytometry. As, asynchronous. (D) Cells were treated as in A. Samples were collected 90 min after release from alpha factor at 30 °C. (E) Exponentially growing cells at 25 °C were transferred to 30 °C for the indicated time and harvested for DNA content analysis by flow cytometry. As, asynchronous. (F) Budding index was assessed 45 and 60 min after release from alpha-factor toward *S* at 30 °C. Cells were treated as in A. At least 100 cells were inspected per condition. (G) Cells were arrested in G1 at 25 °C using alpha factor (alpha) and released toward *S* at 39 °C for 3 h. Cells were then transferred to 30 °C for 30 min before harvest. Samples were taken for DNA content analysis by flow cytometry. (H) Budding index of cells harvested in D. At least 100 cells were inspected per condition.

RIF1 contributes to the phenotypes of *hst3Δ hst4Δ* cells. We next tested the impact of *RIF1* on the phenotypes of *hst3Δ hst4Δ* cells. Interestingly, deletion of *RIF1* rescued the temperature sensitivity of *hst3Δ hst4Δ* cells as well as the synthetic lethality of *hst3Δ hst4Δ sir2Δ* (Fig. 6A), without noticeably affecting H3 K56ac levels (Fig. 6B). We note that for unknown reasons *hst3Δ hst4Δ* cells are temperature sensitive in S288C-derived genetic backgrounds but not in W303 (our unpublished observations; e.g., compare Fig. 5A and Fig. 6A). Because of this, while most of the experiments involving *hst3Δ hst4Δ* were done in W303-derived strains, certain experiments including the one presented in Fig. 6A were done in the BY4741 background (Table 3 indicates the yeast strains used in each figure of this study).

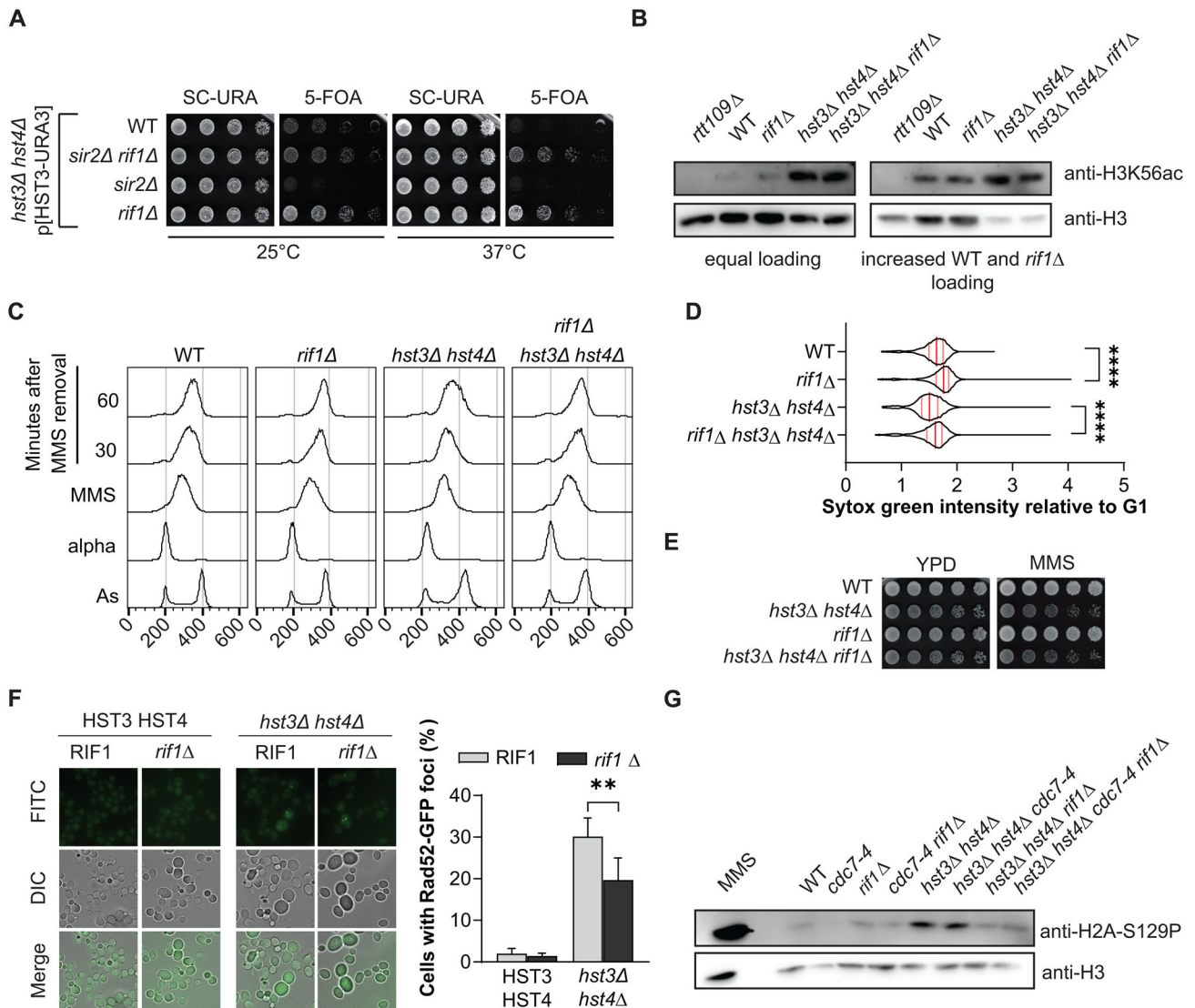


FIG 6 *RIF1* contributes to the phenotypes of *hst3Δ hst4Δ* cells. (A) Five-fold serial dilutions of cell cultures were spotted on solid SC-URA and 5-FOA media and incubated at the indicated temperature. (B) Exponentially growing cells in YPD at 25 °C were harvested and processed for immunoblotting. (C) Cells were arrested in G1 at 25 °C using alpha factor (alpha) and released toward S in medium containing 0.01% of MMS for 90 min (MMS). MMS was inactivated by washing in YPD containing 2.5% sodium thiosulfate, followed by release in fresh YPD. Samples were taken for flow cytometry analysis of DNA content at the indicated time points. As, asynchronous. (D) Violin plot representing the Sytox Green value (DNA content) per cell from the 60 min time point in C normalized to the corresponding G1 median value. Red bars represent the median and pink bars represent the quartiles. *****P* value < 0.0001, unpaired two-tailed Mann–Whitney test. (E) Five-fold serial dilutions of cell cultures were spotted on YPD-agar and YPD-agar containing 0.0025% MMS plates and incubated at 25 °C. (F) The fraction (%) of cells harboring Rad52-GFP foci was assessed by fluorescence microscopy in exponentially growing cells at 25 °C. Left panel: representative microscopy images. Right panel: quantification of cells with Rad52-GFP foci. Graph bars represent the mean value ± SEM of 10 independent cultures. ***P* < 0.01, unpaired two-tailed Student’s *t* test. (G) Exponentially growing cells in YPD at 25 °C were harvested for immunoblotting. MMS: Cells were exposed to 0.03% MMS for 1 h prior to harvesting as control.

We previously demonstrated that transient exposure to methyl methane sulfonate (MMS), an alkylating agent that generates replication-blocking lesions such as 3-methyl adenine, prevents timely completion of S phase in *hst3Δ hst4Δ* cells.²⁴ DNA content flow cytometry analyses revealed that deletion of *RIF1* noticeably rescued the S phase progression delay caused by transient MMS exposure in *hst3Δ hst4Δ* double mutants (Fig. 6C and D), consistent with the notion that Rif1 compromises DNA replication completion in these cells. Nevertheless, deletion of *RIF1* did not rescue the sensitivity of *hst3Δ hst4Δ* to MMS (Fig. 6E), which may be due to the fact that, in addition to its role in regulating origin activity, Rif1 acts to stabilize stalled replication forks.⁴⁹ We also found that *rif1Δ* reduced spontaneous formation of Rad52 foci and histone H2A S129 phosphorylation in *hst3Δ hst4Δ* cells (Fig. 6F and G), indicating that, in the absence of exogenous replicative stress-inducing genotoxins, Rif1 activity causes DNA damage in Hst3/Hst4-deficient cells. The above data, combined with those linking Rif1 to NAM sensitivity, support the notion that Rif1/Glc7-mediated reversal of DDK-dependent phosphorylation, and consequent inhibition of origins of DNA replication, contributes to the phenotypes of cells lacking Hst3 and Hst4.

***cdc7-4 hst3Δ hst4Δ* cells display synthetic defects in the initiation of origins of replication.** We next tested whether *cdc7-4 hst3Δ hst4Δ* cells present synthetic defects in DDK-dependent phosphorylation of MCM subunits and, consequently, initiation of DNA replication. Since a small fraction of total MCM are phosphorylated at any given point during S,⁵⁰ we purified phosphorylated proteins using Pro-Q diamond resin (see Materials and methods) and then quantified MCM4 in the eluate using immunoblotting (Fig. 7A). As anticipated, the levels of MCM4 was higher in the eluate originating from S vs G1 *cdc7-4* cells, reflecting increased phosphorylation; moreover, deletion of *RIF1* further increased S phase MCM4 phosphorylation, as previously documented.^{33,50} Interestingly, we found that deletion of *RIF1* only modestly increased the levels of phosphorylated MCM4 in *cdc7-4 hst3Δ hst4Δ* cells compared to the situation in *cdc7-4*. This suggests that the impact of *hst3Δ hst4Δ* on DNA replication is not strictly dependent on abnormally elevated Rif1-Glc7 activity, but may instead reflect defective MCM phosphorylation/activation by DDK. We nevertheless note that our results clearly indicate that such modest impact of *rif1Δ* on MCM phosphorylation is sufficient to rescue DNA replication progression (e.g., see Fig. 5B).

Formation of replication forks at origins prevents the entry of yeast chromosomes in pulsed-field gel electrophoresis (PFGE) gels.⁵¹ We found that PFGE signals, reflecting entry of chromosomes in the gel, were significantly stronger in *cdc7-4 hst3Δ hst4Δ* cells at 45 and 60 min after release from alpha factor compared to WT, *hst3Δ hst4Δ* and *cdc7-4* (Fig. 7B and C). This is consistent with the notion that a reduced proportion of *cdc7-4 hst3Δ hst4Δ* cells activated origins throughout chromosomes compared to control strains. We next used alkaline gel electrophoresis and Southern blotting to detect formation of low molecular weight nascent DNA at the efficient early origin ARS305, as previously described.⁶ Cells were released from alpha factor arrest at 30 °C in a medium containing the replication-blocking drug hydroxyurea (HU) to limit the extent of DNA replication fork progression at each origin. The results indicate a strong reduction in the amount of low molecular weight DNA formed at ARS305 within 60 min in *cdc7-4 hst3Δ hst4Δ* cells compared to *cdc7-4* (Fig. 7D), consistent with diminished origin activation in *cdc7-4 hst3Δ hst4Δ* mutants.

To further validate these results, we released G1-arrested cells toward S phase at the nonpermissive temperature of 37 °C in the presence of the nucleoside analog BrdU for 60 min, and then switched the temperature of the cultures to 30 °C for 30 min. BrdU-IP followed by quantitative PCR (qPCR) was then used to quantify incorporation of BrdU in genomic DNA at three early origins (ARS305, ARS315 and ARS1211). This analysis revealed that BrdU incorporation into nascent DNA is significantly reduced in *cdc7-4 hst3Δ hst4Δ* compared to *cdc7-4* cells at these early/efficient origins of replication (Fig. 7E to G). Consistently, qPCR analysis on total genomic DNA showed that compared to *cdc7-4* cells, duplication of DNA at these origins was inhibited in *cdc7-4 hst3Δ*

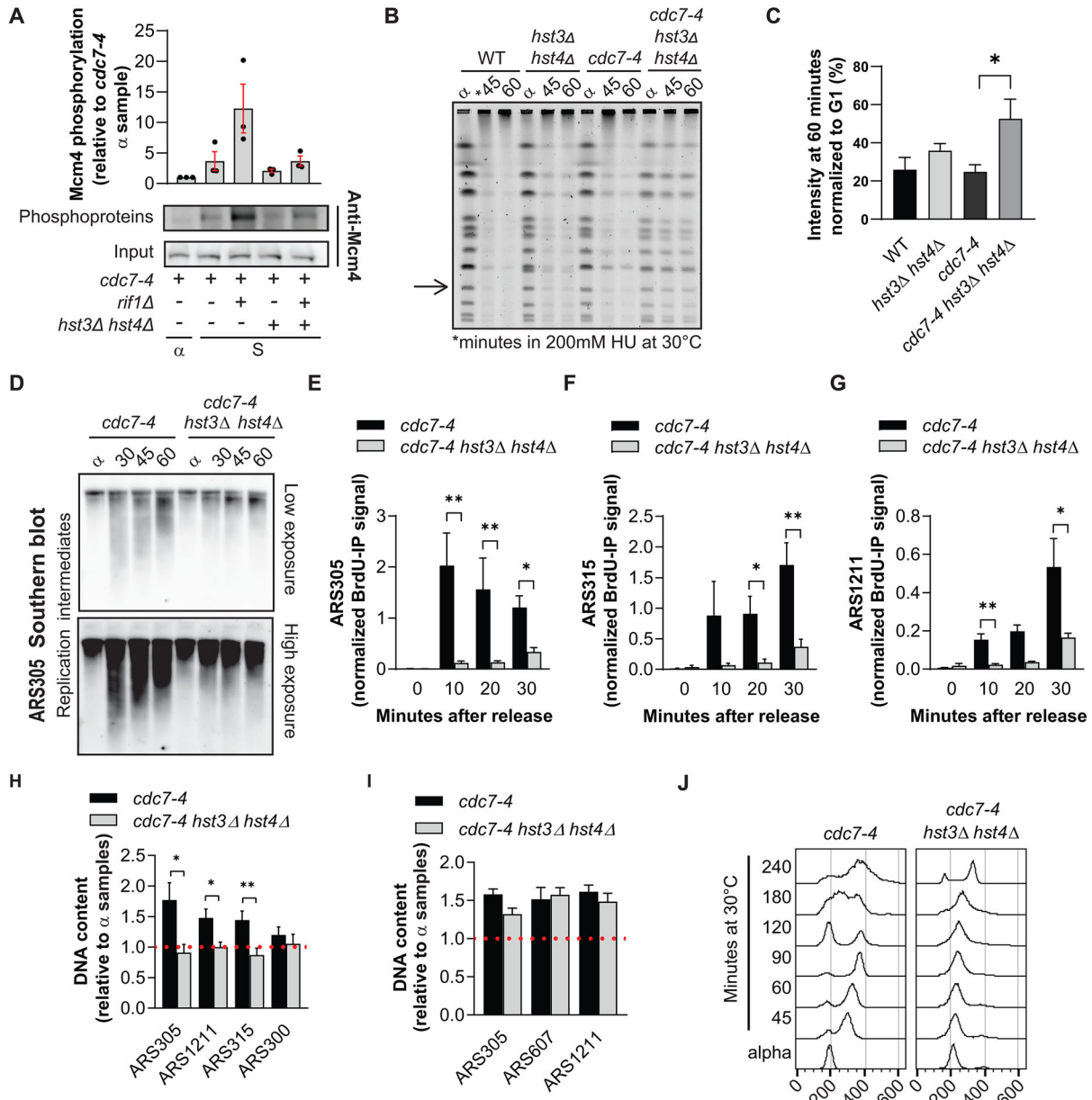


FIG 7 Deletion of *HST3* and *HST4* inhibits the activation of origins of replication in *cdc7-4* cells. (A) Cells were arrested in G1 using alpha factor (α) and released toward S phase for 30 min at 29°C. Cells were collected for phosphoprotein purification followed by immunoblotting (see Materials and Methods). The low abundance of phosphorylated Mcm4 in alpha factor arrested *cdc7-4* cells was used as negative control (α). Bars represent the mean \pm SEM of densitometry quantification of three independent experiments. Representative images of one replicate are shown. (B) Cells were arrested in G1 at 25°C using alpha factor (α) and released toward S phase in the presence of 200 mM HU for the indicated time at 30°C. PFGE was performed as described in Materials and Methods. The arrow indicates the band used for quantification in C. (C) Densitometric quantification of the selected band from B. Bars represent the mean \pm SEM of three independent experiments. (D) Cells were arrested in G1 using alpha factor at 25°C (alpha) and released at 30°C in YPD medium supplemented with 200 mM HU for the indicated time period before harvest. DNA samples were run on alkaline gels followed by Southern blotting to detect short ssDNA fragments generated at ARS305 upon origin activation. (E-G) Cells were arrested in G1 at 25°C using alpha factor and released at 37°C for 1 h. Cells were then incubated at 30°C for 30 min, or at 25°C for 1 h in presence of 200 mM HU before harvest (for normalization purposes, see below). DNA samples were extracted, immunoprecipitated using anti-BrdU antibody and processed for quantitative PCR analysis. Bars represent the mean \pm SEM of the percent of the input of five independent experiments using qPCR primers for the early origins (E) ARS305, (F) ARS315, and (G) ARS1211. Normalization for BrdU intake capacity per strain was performed by incubating cells at the permissive temperature of 25°C for 1 h in the presence of 200 mM HU as described in Materials and Methods. (H) Cells were arrested in G1 using alpha factor at 25°C and released toward S for 1 h. Cells were then incubated at 30°C for 30 min before harvest. DNA was extracted and processed for quantitative PCR analysis (see Methods). qPCR signal for a given origin was normalized to that obtained from the *NegV* locus (which is expected to remain unreplicated 30 min postrelease from G1 toward S), and then divided by the normalized signals obtained from alpha-factor arrested (G1) cells. Graph bars represent mean \pm SEM of five independent experiments. (I) qPCR analysis of DNA content at selected origins. Indicated strains were treated as in G, except that cells were released toward S phase in presence of 200 mM HU for 120 min at 30°C before harvest. Graph bars represent mean \pm SEM of three independent experiments. (J) Cells were arrested in G1 using alpha factor (alpha) at 25°C and released toward S phase at 30°C for the indicated time. Samples were taken for DNA content analysis by flow cytometry. As, asynchronous. Throughout this figure, * $P < 0.05$ and ** $P < 0.01$, unpaired two-tailed Student's *t* test.

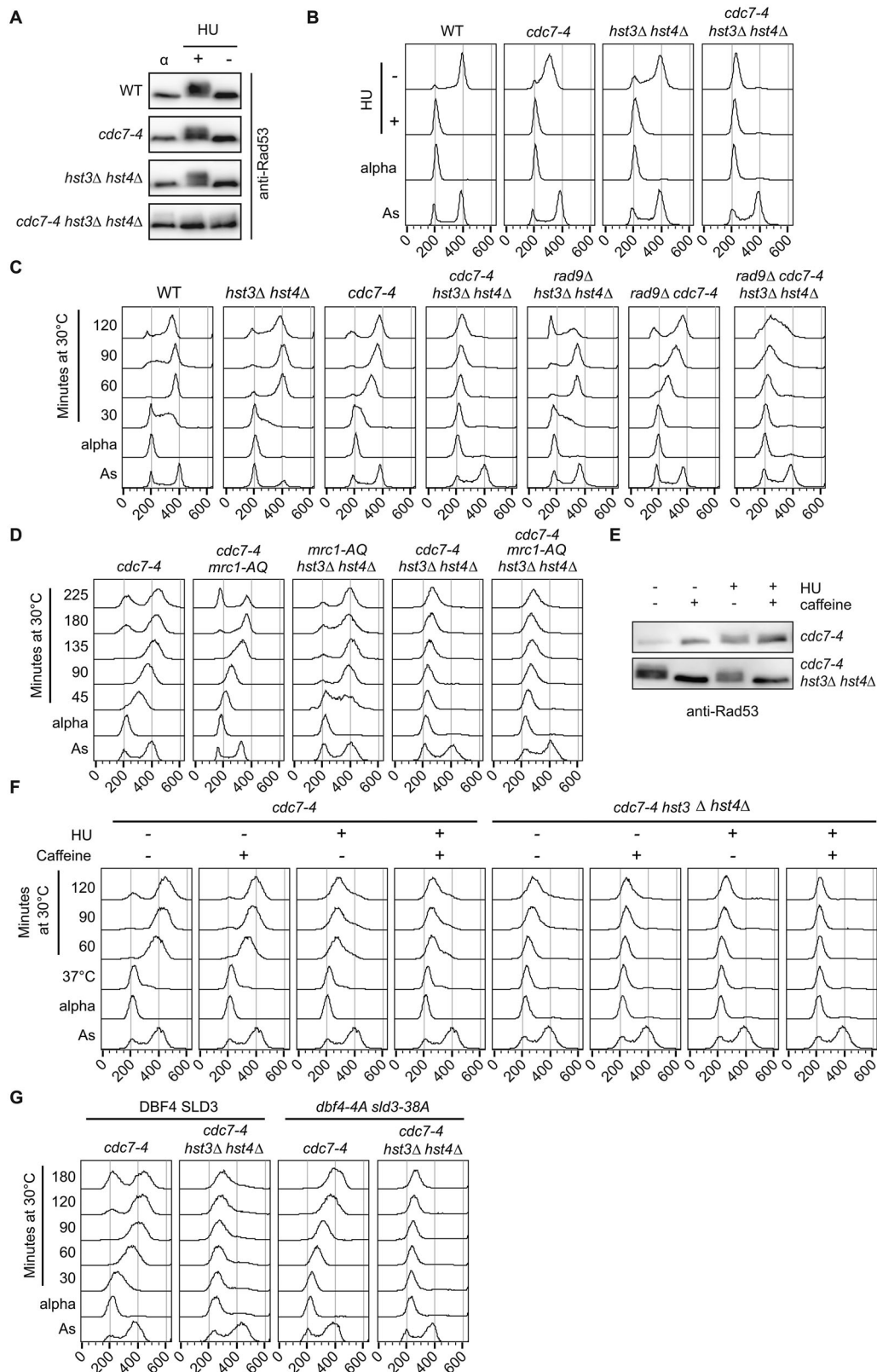


FIG 8 The DNA replication defects of *cdc7-4 hst3Δ hst4Δ* cells are not due to elevated Rad53 activation in early S phase. (A–B) Cells were arrested in G1 at 25°C using alpha factor (alpha) and released toward S phase at 30°C in the presence or absence of 200 mM HU. Cells were harvested 60 min postrelease toward S and processed for immunoblotting (A) and DNA content analysis by flow cytometry (B). As, asynchronous. (C) Cells were arrested in G1 at 25°C using alpha factor (alpha) and released toward S phase at 30°C. Samples were taken for DNA content analysis by flow cytometry. As, asynchronous. (D) DNA content analysis by flow cytometry. Cells were treated as in C. (E–F) Cells were treated as in C except that releases toward S phase at 30°C were done in YPD ± 200 mM HU ± 0.15% caffeine. After 60 min of release, cells were harvested for immunoblotting (E). DNA content was assessed by flow cytometry using samples harvested at the indicated time points (F). (G) DNA content analysis by flow cytometry. Cells were treated as in C.

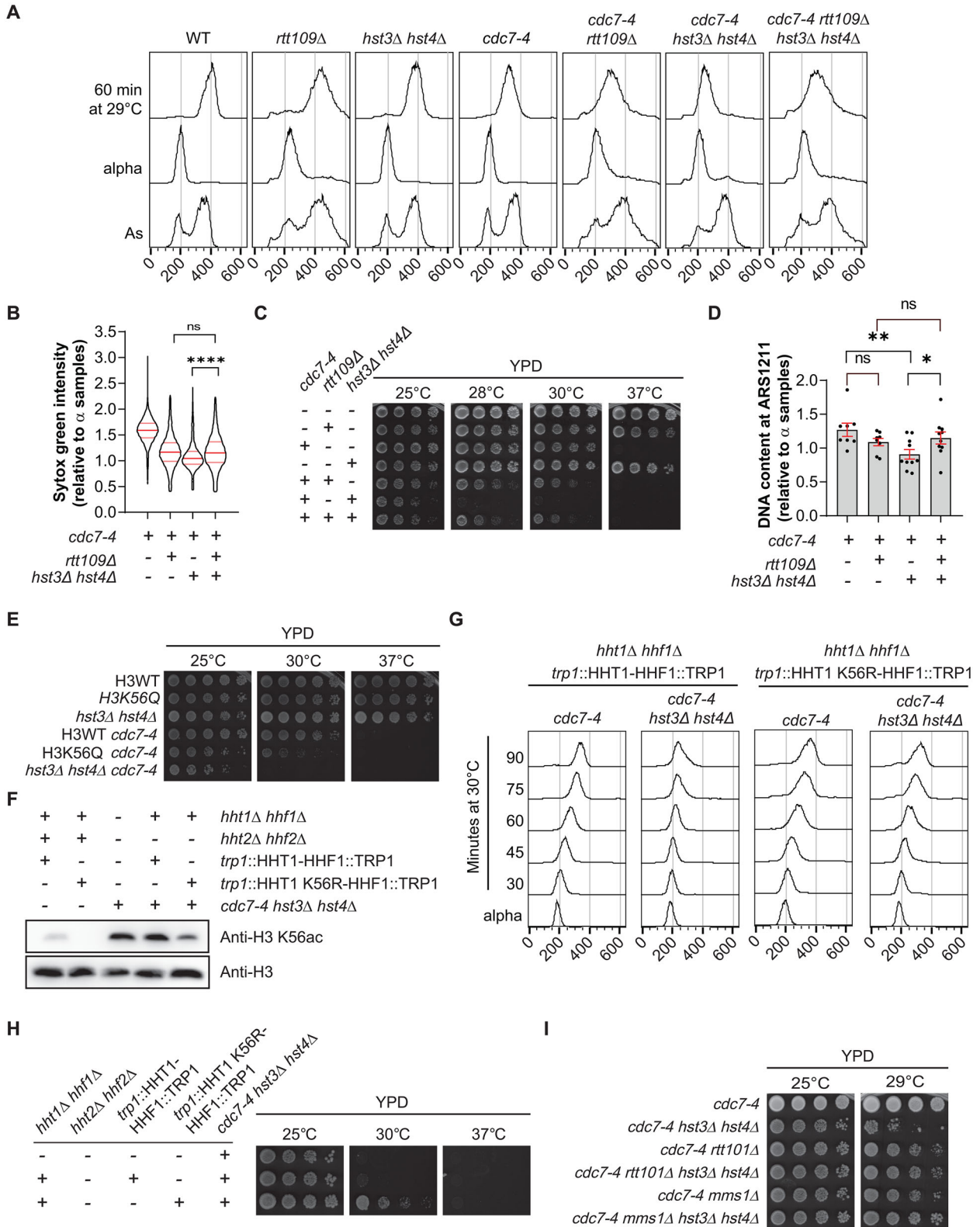


FIG 9 Constitutive H3 K56 acetylation, Rtt101, and Mms1 cause S phase progression defects and synthetic temperature sensitivity in *cdc7-4 hst3Δ hst4Δ* cells. (A–B) Cells were arrested in G1 at 25°C using alpha factor (alpha) and released toward S for the indicated time period at 29°C. Samples were taken for DNA content analysis by flow cytometry. As, asynchronous. (B) Violin plot represents the Sytox green value (DNA content) per cell from the 60 min time point in A normalized to the corresponding G1 median value. Red bars represent the median and pink bars represent the quartiles. ns, $P > 0.05$ and **** $P < 0.0001$, unpaired two-tailed Mann–Whitney test. (C) Five-fold serial dilutions of cell cultures were spotted on YPD-agar plates. Plates were incubated at the indicated temperature. (D) Asynchronously growing cells were arrested in G1 using alpha factor at 25°C. Cells were then released toward S phase at 29°C for 60 min in presence of 200 mM HU before harvest. DNA was extracted and processed for quantitative PCR analysis (see Materials and

hst4Δ mutants 30 min after release from alpha factor arrest at 30 °C (Fig. 7H). We note that *cdc7-4 hst3Δ hst4Δ* cells eventually initiated DNA replication and completed S phase when incubated for extended periods at 30 °C (240 min postrelease from alpha factor arrest; Fig. 7I and J). Taken together, the results indicate that the *hst3Δ hst4Δ* mutations cause synthetic defects in the activation of replication origins when combined with *cdc7-4*, thereby strongly delaying S phase progression at 30 °C.

Inhibition of origin activity in *cdc7-4 hst3Δ hst4Δ* cells is not due to activation of Rad53 in early S phase. One of the key roles of intra-S phase checkpoint signaling is to limit the activation of origins in response to DNA replication stress.^{6,52} In yeast, this has been shown to occur via Rad53-dependent phosphorylation and consequent inactivation of Dbf4 and Sld3.⁷ Cells lacking Hst3/Hst4 activity are known to present spontaneous DNA damage and constitutive activation of Rad53.^{19,23,24,26,27} We therefore investigated the possible influence of Rad53 activity on the S phase progression delay observed in *cdc7-4 hst3Δ hst4Δ* cells. While *cdc7-4 hst3Δ hst4Δ* cells constitutively present some levels of Rad53 phosphorylation in G1, no obvious elevation in Rad53 autophosphorylation-induced electrophoretic mobility shift was observed upon release of cells from alpha factor arrest toward S phase at 30 °C either in the presence or absence of HU (Fig. 8A and B). This result is consistent with the notion that few if any replication forks are progressing in these conditions, thereby reducing the number of stalled replication forks in HU-treated or untreated conditions and diminishing Rad53 activation.

We next tried to delete *RAD53* and *SML1* in *cdc7-4 hst3Δ hst4Δ* cells to directly assess the role of intra-S phase checkpoint signaling on the phenotypes of these mutants; *SML1* deletion is necessary to permit viability of *rad53Δ* mutants.⁵³ However, even though *hst3Δ hst4Δ rad53Δ sml1Δ* cells are viable,²³ we failed to generate a *cdc7-4 hst3Δ hst4Δ rad53Δ sml1Δ*, suggesting that for unknown reason this combination of mutations causes synthetic lethality. To circumvent this, we engineered *cdc7-4 hst3Δ hst4Δ* strains harboring mutations in *RAD9* and *MRC1*, two key mediators of the activation of the intra-S phase checkpoint.⁵ We found that deletion of *RAD9* in *cdc7-4 hst3Δ hst4Δ* cells led to modest improvement in S phase progression, but only after 60 min of release from alpha factor arrest (Fig. 8C). This suggests that Rad9 might contribute to the long-term maintenance, rather than the establishment, of the S phase progression defects observed in *cdc7-4 hst3Δ hst4Δ* cells. In contrast, expression of a mutated allele of *Mrc1* (*mrc1-AQ*), which compromises its role in activating intra-S phase checkpoint kinases,⁵⁴ did not have any influence on S phase progression in *cdc7-4 hst3Δ hst4Δ* cells (Fig. 8D).

We further found that while inhibition of the apical kinase of the intra-S phase checkpoint Mec1 using caffeine completely abrogated Rad53 phosphorylation,^{55,56} as expected, such treatment did not rescue the strong inhibition of DNA replication progression of *cdc7-4 hst3Δ hst4Δ* mutants (Fig. 8E and F). We also note that caffeine did not prevent *cdc7-4* cells from completing DNA replication at 30 °C (Fig. 8F). Expression of Dbf4 and Sld3 variants that cannot be phosphorylated by Rad53 was previously shown to abrogate intra-S phase checkpoint-dependent inhibition of origin activity in yeast.⁷ We found that introducing such mutated alleles of *DBF4* and *SLD3* in *cdc7-4 hst3Δ hst4Δ* cells does not alleviate their S phase progression defects at 30 °C; importantly, mutations of *DBF4* and *SLD3* did not prevent *cdc7-4* cells from completing S phase in these conditions (Fig. 8G). We conclude that the incapacity of *cdc7-4 hst3Δ hst4Δ* mutants to initiate DNA replication when released from G1 at 30 °C is not due to

FIG 9 Legend (Continued)

Methods). qPCR signal for ARS1211 was normalized to that obtained from the *NegV* locus, and then divided by the normalized signals obtained from corresponding alpha-factor arrested cells. Graph bars represent mean ± SEM of more than eight independent experiments. Ns, false discovery rate (FDR)-adjusted $P > 0.05$, *FDR-adjusted $P < 0.05$ and **FDR-adjusted $P < 0.01$, P values were calculated using unpaired multiple t test analysis and FDR (Benjamini, Krieger, and Yekutieli method). (E) As in C. (F) Exponentially growing cells at 25 °C were processed for immunoblotting. (G) Asynchronously growing cells were arrested in G1 using alpha factor (alpha) at 25 °C. Cells were then released toward S phase at 30 °C for the indicated time period before harvest. Samples were processed for DNA content analysis by flow cytometry. (H) As in C. (I) As in C.

rapid elevation of Rad53-dependent phosphorylation of Sld3 and Dbf4 in early S and consequent inhibition of origins of replication.

Constitutive histone H3 lysine 56 acetylation causes replication defects in *cdc7-4* cells. Constitutive acetylation of H3 K56 causes most of the severe phenotypes associated with *hst3Δ hst4Δ* mutants, including their temperature and DNA damage sensitivity.^{19,22,23} While H3 K56ac strictly depends on the Rtt109 histone acetyltransferase,⁴² this enzyme also acetylates other residues in the N-terminal tail of histone H3,^{20,57,58} although there are currently no evidence that link the acetylation of these residues with the phenotypes of *hst3Δ hst4Δ* mutants. We found that deletion of *RTT109* significantly rescued DNA replication progression and proliferation of *cdc7-4 hst3Δ hst4Δ* cells at a semipermissive temperature for *cdc7-4* (Fig. 9A to C). Similarly, we found that the initiation of DNA replication at the early origin ARS1211, as measured by qPCR-based quantification of DNA duplication at this locus, was rescued in *cdc7-4 hst3Δ hst4Δ rtt109Δ* compared to *cdc7-4 hst3Δ hst4Δ* cells (Fig. 9D).

To test whether hyperacetylation of H3 K56 per se is responsible for the replication defects observed in *hst3Δ hst4Δ cdc7-4* cells, we replaced histone H3 by a H3 K56Q variant to mimic constitutive H3 K56ac in *cdc7-4* cells; such combination of mutations caused strong synthetic temperature sensitivity (Fig. 9E). We next sought to engineer a *cdc7-4 hst3Δ hst4Δ* strain lacking H3 K56ac via expression of a histone H3 variant in which lysine 56 is replaced by a nonacetylatable arginine residue (H3 K56R). To this end, both copies of the endogenous genes encoding histone H3 (*HHT1* and *HHT2*) were deleted while one copy of the *HHT1* gene ± K56R mutation was integrated at the *TRP1* locus. We failed to generate the *cdc7-4 hst3Δ hst4Δ* cells expressing either H3 WT or H3 K56R using this standard strategy, suggesting that abnormal histone gene dosage due to deletion of *HHT2* may be lethal in this context. To specifically reduce H3 K56ac levels while minimizing changes in histone gene dosage, we instead replaced *HHT1* by either a WT or K56R allele and left the endogenous copy of *HHT2* intact (Fig. 9F to H). This produced viable *cdc7-4 hst3Δ hst4Δ* strains in which H3 K56ac levels are either unchanged (H3 WT) or noticeably reduced (H3 K56R; Fig. 9F). We observed a rescue of both S phase progression at semirestrictive temperature and of the synthetic temperature sensitivity of *cdc7-4 hst3Δ hst4Δ* upon expression of H3 K56R (compared to control cells expressing H3 WT; Fig. 9G and H). Taken together, the results indicate that constitutive Rtt109-dependent H3 K56ac underlies the synthetic temperature sensitivity and DNA replication defects of *cdc7-4 hst3Δ hst4Δ* cells.

Genetic and biochemical data indicate that Rtt109 and H3 K56ac act at least in part by modulating the activity of a ubiquitin ligase complex composed of the Rtt101, Mms1 and Mms22 subunits.^{59–62} Deletion of the genes encoding subunits of this complex partially suppresses the phenotypes of *hst3Δ hst4Δ* cells,⁵⁹ although the precise mechanisms linking constitutive acetylation of nucleosomal H3 K56ac with Rtt101/Mms1/Mms22 is incompletely characterized. We found that deletion of either *RTT101* or *MMS1* suppressed the synthetic temperature sensitivity of *cdc7-4 hst3Δ hst4Δ* mutant cells (Fig. 9I). In contrast, we were unable to generate *cdc7-4 hst3Δ hst4Δ mms22Δ* cells, suggesting that synthetic lethal interactions between these genes prevent viability. Nevertheless, our results implicate Rtt101-Mms1-containing complexes in H3 K56ac-dependent modulation of DNA replication origins.

DISCUSSION

In yeast, virtually all new histones H3 are acetylated on K56, leading to a chromosome-wide wave of H3 K56ac during S phase.^{19,42} This modification promotes timely formation of nucleosomes behind replication forks by favoring the interaction of new histones with the chromatin assembly factors CAF1 and Rtt106.⁶³ While this “pre-deposition” function of H3 K56ac is well-established, several observations suggest that this mark also plays important biological roles following its incorporation into chromatin.⁶⁴ Constitutive nucleosomal H3 K56ac causes spontaneous DNA damage and extreme sensitivity to replication-blocking drugs in *hst3Δ hst4Δ* cells, suggesting that

chromatin-associated H3 K56ac influences the cellular response to replicative stress.^{22,23} Moreover, cells have evolved molecular mechanisms to degrade Hst3 in response to replicative stress,^{43,65} which raises the possibility that the ensuing persistence of H3 K56ac may somehow contribute to the DNA damage response. Nevertheless, while a multitude of cellular pathways have been associated with nucleosomal H3 K56ac,^{23,24,26,27,59} the molecular basis of the sensitivity of *hst3Δ hst4Δ* mutants to replicative stress, as well as the role of H3 K56ac persistence after DNA damage, are poorly understood.

We previously showed that NAM-induced inhibition of Hst3 and Hst4 causes replicative stress by elevating H3 K56ac.^{26,27} In accord with this, our current and previously published screens revealed that several genes conferring NAM resistance participate in DNA replication and repair (Fig. 1C and D).²⁶ Interestingly, the current screen also revealed that lack of *TAF5* and *TAF12*, which encodes proteins shared by TFIID and the SAGA acetyltransferase complex, strongly sensitizes cells to NAM. Since the SAGA complex modulates the expression of stress-responsive genes,⁶⁶ we speculate that the presence of subunits of this complex among the “hits” of our screen might reflect transcriptional activation of critical cellular stress responses pathways during NAM treatment. Our screen also identified genes involved in proteasome regulation and ubiquitin-dependent processes as modulators of NAM sensitivity (Fig. 1C). As mentioned previously, the Rtt101-Mms1-Mms22 ubiquitin ligase complex displays clear genetic links with H3 K56ac in the context of the response to replicative stress.^{59–62} It is therefore possible that heterozygosity in genes involved in ubiquitin- and proteasome-related processes elevate cell fitness upon NAM-induced inhibition of Hst3 and Hst4 by influencing Rtt101-Mms1-Mms22-related mechanisms.

Published reports indicate that *hst3Δ* cells display H3 K56ac-dependent defects in the maintenance of a chromosome harboring a reduced number of replication origins,^{28,67} which suggests that elevated H3 K56ac might negatively influence the completion of chromosomal DNA replication in situations where the number of active origins is limited. In accord with this, our data indicate that (i) cells harboring hypomorphic alleles of the critical origin activation genes *CDC7* and *DBF4* display strong growth defects in the presence of NAM, and (ii) firing of early/efficient origins of DNA replication is compromised in *cdc7-4 hst3Δ hst4Δ* cells released from G1 toward S at the semi-permissive temperature for *cdc7-4*. Intriguingly, lack of Hst3 alone was insufficient to detectably compromise DNA replication in *cdc7-4* mutants; it is possible that the limited increase of H3 K56ac during G2/M caused by the absence of Hst3 gives rise to subtle replication defects whose detection is facilitated by the use of plasmid stability assays.

Importantly, deletion of *RIF1* alleviated the phenotypes of *cdc7-4* with regard to NAM sensitivity, in agreement with the known role of Rif1 in promoting Glc7-dependent dephosphorylation of MCM complexes leading to inhibition of origin activation.³³ This is also in line with the fact that homozygous deletion of *RIF1* improved cell fitness in response to NAM in our previously published screen.²⁶ Importantly, data presented here also show that lack of Rif1 suppresses several phenotypes of *hst3Δ hst4Δ* cells. While these results can be considered surprising in light of the fact that Rif1 has also been reported to promote the stability of stalled replication forks,⁴⁹ it is possible that the elevation of origin activity caused by *rif1Δ* overrides the negative impact on replicative stress responses caused by this mutation in *hst3Δ hst4Δ* cells. Importantly, our data also indicate that MCM4 phosphorylation is only modestly increased in the absence of *RIF1* in *hst3Δ hst4Δ cdc7-4* cells, suggesting that decreased activation of origin may primarily reflect reduced MCM phosphorylation rather than abnormally elevated Rif1-dependent dephosphorylation of this complex. While the precise mechanism has not been identified, several possibilities exist, including decreased activity/stability/levels of Cdc7-Dbf4 in the presence of constitutive H3 K56ac and/or impaired phosphorylation of Mcm4 due to reduced loading of Mcm4 at origins or inadequate conformation of the protein complex. Further experiments will be required to

explore the precise mechanisms underlying the reduction in Mcm4 phosphorylation caused by the *hst3Δ hst4Δ* mutations.

Replication forks stalling activates Rad53, which then phosphorylates the replication proteins Dbf4 and Sld3 to inhibit the firing of replication origins that have not yet been activated.⁷ In apparent contrast to our results, a previously published report revealed that *hst3Δ hst4Δ* cells present elevated activation of late origins in cells released from G1 toward S phase in medium containing the replication-blocking ribonucleotide reductase inhibitor HU.¹¹ However, such effect was not specific to *hst3Δ hst4Δ* mutants; indeed, this was found to be an indirect consequence of increased spontaneous DNA damage and constitutive Rad53 activity in various replicative stress response mutants, leading to Rad53-dependent elevation of dNTP pools and consequent HU-resistant DNA synthesis.⁶⁸ In contrast, several observations presented here indicate that constitutive H3 K56ac influences origin firing in a manner that does not depend on ongoing Rad53 activity and/or phosphorylation of Sld3 and Dbf4 in early S phase. First, *cdc7-4 hst3Δ hst4Δ* cells do not display noticeable elevation in Rad53 phosphorylation when released from G1 arrest toward S phase at the semipermissive temperature for *cdc7-4*, even in the presence of HU. Second, mutations in *RAD9* or *MRC1*, or treatments that compromise Rad53 activation (caffeine), do not rescue defective S phase progression in *cdc7-4 hst3Δ hst4Δ* mutants. Third, mutations in the genes encoding Sld3 and Dbf4 that abrogate their phosphorylation by Rad53 do not improve DNA replication progression in *cdc7-4 hst3Δ hst4Δ* cells. Taken together, the above data argue that the impact of constitutive H3 K56ac on origin activity in early S phase does not require prior replication forks stalling and ensuing elevation in Rad53 activity. Consistently, we also showed that the activation of several early/efficient origins is strongly delayed in *cdc7-4 hst3Δ hst4Δ* after release from G1 at the semipermissive temperature for *cdc7-4*. Such reduction in the number of progressing replication forks presumably explains why HU exposure does not elevate Rad53 phosphorylation in these conditions.

Our data and those of others argue that elevated H3 K56ac strongly inhibits DNA replication under conditions of reduced DDK activity or in situations where the number of active origins is limited.^{28,67} Such conditions are met in *cdc7-4* or *dbf4-1* mutants at the semipermissive temperature, or in cells harboring an artificial chromosome engineered to have a low number of origin. As mentioned earlier, replication forks stalling leading to Rad53 activation and consequent phosphorylation of Dbf4 also strongly diminishes DDK activity during S phase.⁷ It is therefore possible that genotoxin-induced replication forks stalling and consequent Rad53 activation might synergize with constitutive H3 K56ac in inhibiting late origin activity in *hst3Δ hst4Δ* cells, even in the presence of a wild-type allele of *CDC7*. In turn, this would be expected to compromise the completion of DNA replication, eventually leading to cell death. In agreement with this, we and others previously showed that (i) *hst3Δ hst4Δ* cells cannot complete DNA replication in a timely manner after transient exposure to genotoxic drugs during S phase,²⁴ (ii) *hst3Δ hst4Δ* cells present persistent activation of Rad53 upon DNA damage,^{23,24,26} (iii) limiting Rad53 activation partially rescues the phenotypes of *hst3Δ hst4Δ* mutants^{23,24,26,69}, and (iv) elevating the firing of late origins of replication by overexpression of Cdc45, Sld3 and Sld7 can rescue certain phenotypes caused by elevated H3 K56ac.^{27,69} The combined negative effects of Rad53 activation and elevated H3 K56ac on origin activity would be expected to force replication forks to travel unusually long distances before encountering a converging fork. Consequently, a substantial fraction of persistently stalled replication forks would not be “rescued” by converging forks in these conditions, leading to under-replicated chromosomal regions, replication forks collapse, DNA damage, and eventual arrest in G2/M, which are all observed in *hst3Δ hst4Δ* cells.^{12,19,23,24}

While the precise mechanism linking H3 K56ac to origin activity is unclear, we demonstrated that deletion of *RTT101* or *MMS1*, which encode subunits of a ubiquitin ligase complex previously genetically linked to H3 K56ac,^{59,60} rescues the synthetic

temperature sensitivity of *hst3Δ hst4Δ cdc7-4*. Since *rtt101Δ* and *mms1Δ* do not influence H3 K56ac levels,⁵⁹ any models involving only H3 K56ac-dependent modulation of chromatin structure per se are unlikely to explain the impact of this modification on origin activity. We note that Rtt101 recruitment to chromatin upon DNA damage was shown to depend at least partly on the H3 K56 acetyltransferase Rtt109.⁶² Moreover, Mms1 has been reported to interact directly with the origin recognition complex subunit Orc5,⁷⁰ although the biological relevance of this interaction has not been characterized. The above considerations raise the possibility that DNA damage-induced persistence of H3 K56ac might modulate Rtt101/Mms1 activity in trans to downregulate origin activity. Further experiments will be required to test the validity of such models, and to precisely ascertain the mechanistic basis of the impact of H3 K56ac on DNA replication dynamics.

MATERIALS AND METHODS

Yeast strains and growth conditions. Yeast strains used in this study are listed in Table 3 and were generated and propagated using standard yeast genetics methods. Yeast strains used in Figure 1D and Table S1 (supplementary material) were from the BY4743 heterozygote yeast deletion collection (ThermoFisher). For nicotinamide (NAM) treatments, asynchronously growing cells were centrifuged and resuspended at 0.01–0.1 OD/mL in YPD or synthetic (SC) medium containing 20 mM NAM (Sigma-Aldrich). Cells were incubated on a shaker for indicated time. Cell synchronization in G1 was performed by incubating MATa yeasts in medium containing 2 μg/mL alpha-factor for 90 min followed by the addition of a second dose of 2 μg/mL of alpha-factor for another 75 min. Cells were then washed once in YPD or SC medium and released in S phase in medium supplemented with 5 μg/mL pronase (protease from *Streptomyces griseus*, Sigma-Aldrich). For nocodazole arrest, cells were incubated in a medium containing 15 μg/mL nocodazole (Cell Signaling) for 2 h when starting with asynchronous cells or for 90 min in the case of cells previously synchronized in G1 using alpha factor. Cells were then washed once in YPD medium. Release conditions are indicated in figure legends. For ionizing irradiation, exponentially growing cells were exposed to 40 Gy followed by a 60-min incubation at 30 °C prior to sample collection. For methyl methanesulfonate (MMS) treatment, cells were first synchronized in G1 using alpha factor, then incubated in YPD containing 0.01% MMS (Sigma-Aldrich) and 5 μg/mL pronase at a density of 1 OD₆₃₀/mL for 60 min. After treatment, cells were washed twice with YPD containing 2.5% sodium thiosulfate (Bioshop), followed by incubation in YPD. Caffeine (Sigma-Aldrich) was used at a concentration of 0.15%.

Genome-wide fitness screen. The heterozygote diploid yeast fitness screen was realized as previously described.^{71–73} Briefly, pools of the yeast heterozygote diploid deletion mutant collection (BY4743 background) were incubated at 30 °C in YPD ± 41 mM NAM. Cells were collected after 20 generations. PCR reactions were performed on extracted DNA to amplify sequence barcodes, and products were used to probe high-density oligonucleotide Affymetrix TAG4 DNA microarrays. Hybridization, washing, staining, scanning and intensity values calculation were performed as previously described.^{71–73} For Z-score calculation, the intensity value of each mutant was divided by the standard deviation. The gene ontology (GO) term finder tool from the Saccharomyces Genome Database (www.yeastgenome.org) was used to identify cellular processes affected by NAM treatment.^{74,75} Processes identified were considered significant if *P*-values ≤ 0.01. The REViGO tool was then used to summarize significant GO-terms identified by removing redundant ones.⁷⁶ Top 1% genes (Z-score > 2.58 or < -2.58) were compared to a previously published screen (performed on homozygote diploid mutants) using Venn diagrams.²⁶

Competitive growth assay. 0.0005 OD₆₃₀ of heterozygous deletion and WT diploid yeast cultures were mixed and incubated in YPD ± 41 mM NAM at 25 °C in a 96-well plate. Throughout the incubation, OD₆₃₀ were taken and cells were diluted appropriately to prevent saturation of the culture. After 20 generations, 0.01 OD₆₃₀ of cells was spread on YPD-agar ± G418 plates. Plates were incubated at 30 °C for 48 h and colonies were then counted. The following formula was used to describe growth ± NAM:

$$\frac{((\text{NAM} : \text{G418})/(\text{NAM} : \text{YPD}))}{((\text{YPD} : \text{G418})/(\text{YPD} : \text{YPD}))}$$

where NAM:G418 is the number of colonies from cells that were grown in YPD + 41 mM NAM and then plated on YPD + 200 μg/mL G418, NAM:YPD is the number of colonies from cells grown on YPD + 41 mM NAM and then plated on YPD, YPD:G418 is the number of colonies from cells grown on YPD and then plated on YPD + 200 μg/mL G418, YPD:YPD is the number of colonies from cells grown on YPD and then plated on YPD.

Yeast growth assays. For growth in liquid medium, cells were grown to saturation in YPD in a 96-well plate. Cells were then diluted in fresh medium to 0.0005 OD₆₃₀/ml in 100 μL of YPD containing appropriate concentrations of NAM (Sigma-Aldrich). Cells were then incubated at the indicated temperature for 48–72 h. OD₆₃₀ was determined using a Biotek EL800 plate reader equipped with Gen5 version 1.05 software. Wells containing YPD were used as blanks. For spot growth assays on solid media, cells were grown in YPD or SC medium in a 96-well plate to equivalent OD₆₃₀. Cells were serially diluted 1:5 and spotted on YPD medium containing nicotinamide (Sigma-Aldrich), methyl methanesulfonate (Sigma-Aldrich), hydroxyurea (BioBasics), or SC medium depleted of uracil (SC-URA) or SC-URA medium

TABLE 3 Yeast strains used in this study

Strain name	Genotype	Figure	Reference
ASY2370	BY4743 MATa/ α <i>his3Δ1/his3Δ1 leu2Δ0/leu2Δ0 LYS2/lys2Δ0 met15Δ0/MET15 ura3Δ0/ura3Δ0</i>	1D	This study
RTY5970	BY4743 MATa/ α <i>ura3Δ0 leu2Δ0 his3Δ1 lys2Δ0/LYS + met15Δ0/MET15+ can1Δ::LEU2+-MFA1pr-HIS3/CAN1+ cdc6Δ::KANMX/CDC6</i>	1D	Het. Diploid yeast collection
RTY5972	BY4743 MATa/ α <i>ura3Δ0 leu2Δ0 his3Δ1 lys2Δ0/LYS + met15Δ0/MET15+ can1Δ::LEU2+-MFA1pr-HIS3/CAN1+ cdc7Δ::KANMX/CDC7</i>	1D	Het. Diploid yeast collection
RTY5980	BY4743 MATa/ α <i>ura3Δ0 leu2Δ0 his3Δ1 lys2Δ0/LYS + met15Δ0/MET15+ can1Δ::LEU2+-MFA1pr-HIS3/CAN1+ dbf4Δ::KANMX/DBF4</i>	1D	Het. Diploid yeast collection
RTY5984	BY4743 MATa/ α <i>ura3Δ0 leu2Δ0 his3Δ1 lys2Δ0/LYS + met15Δ0/MET15+ can1Δ::LEU2+-MFA1pr-HIS3/CAN1+ orc5Δ::KANMX/ORC5</i>	1D	Het. Diploid yeast collection
RTY5976	BY4743 MATa/ α <i>ura3Δ0 leu2Δ0 his3Δ1 lys2Δ0/LYS + met15Δ0/MET15+ can1Δ::LEU2+-MFA1pr-HIS3/CAN1+ rfa1Δ::KANMX/RFA1</i>	1D	Het. Diploid yeast collection
RTY5978	BY4743 MATa/ α <i>ura3Δ0 leu2Δ0 his3Δ1 lys2Δ0/LYS + met15Δ0/MET15+ can1Δ::LEU2+-MFA1pr-HIS3/CAN1+ rfa2Δ::KANMX/RFA2</i>	1D	Het. Diploid yeast collection
RTY5974	BY4743 MATa/ α <i>ura3Δ0 leu2Δ0 his3Δ1 lys2Δ0/LYS + met15Δ0/MET15+ can1Δ::LEU2+-MFA1pr-HIS3/CAN1+ sld3Δ::KANMX/SLD3</i>	1D	Het. Diploid yeast collection
RTY6000	BY4743 MATa/ α <i>ura3Δ0 leu2Δ0 his3Δ1 lys2Δ0/LYS + met15Δ0/MET15+ can1Δ::LEU2+-MFA1pr-HIS3/CAN1+ slx4Δ::KANMX/SLX4</i>	1D	Het. Diploid yeast collection
RTY6002	BY4743 MATa/ α <i>ura3Δ0 leu2Δ0 his3Δ1 lys2Δ0/LYS + met15Δ0/MET15+ can1Δ::LEU2+-MFA1pr-HIS3/CAN1+ pph3Δ::KANMX/PPH3</i>	1D	Het. Diploid yeast collection
RTY5994	BY4743 MATa/ α <i>ura3Δ0 leu2Δ0 his3Δ1 lys2Δ0/LYS + met15Δ0/MET15+ can1Δ::LEU2+-MFA1pr-HIS3/CAN1+ yku70Δ::KANMX/YKU70</i>	1D	Het. Diploid yeast collection
RTY5996	BY4743 MATa/ α <i>ura3Δ0 leu2Δ0 his3Δ1 lys2Δ0/LYS + met15Δ0/MET15+ can1Δ::LEU2+-MFA1pr-HIS3/CAN1+ srs2Δ::KANMX/SRS2</i>	1D	Het. Diploid yeast collection
RTY5988	BY4743 MATa/ α <i>ura3Δ0 leu2Δ0 his3Δ1 lys2Δ0/LYS + met15Δ0/MET15+ can1Δ::LEU2+-MFA1pr-HIS3/CAN1+ taf5Δ::KANMX/TAF5</i>	1D	Het. Diploid yeast collection
RTY5990	BY4743 MATa/ α <i>ura3Δ0 leu2Δ0 his3Δ1 lys2Δ0/LYS + met15Δ0/MET15+ can1Δ::LEU2+-MFA1pr-HIS3/CAN1+ taf12Δ::KANMX/TAF12</i>	1D	Het. Diploid yeast collection
HWY3774	W303 MATa <i>ade2-1 trp1-1 can1-100 leu2-3,112 his3-11,15 ura3Δ GAL psi + bar1Δ GAL-MHT</i>	2A, B	11
HWY3777	W303 MATa <i>ade2-1 trp1-1 can1-100 leu2-3,112 his3-11,15 ura3Δ GAL psi + bar1Δ dbf4-1 GAL-MHT</i>	2A, B, E	11

(Continued)

TABLE 3 (Continued).

Strain name	Genotype	Figure	Reference
RTY6124	W303 MAT α <i>ade2-1 ura3-1 his3-11,15 leu2-3-112 trp1-1 can1-100</i>	2A, C, D	This study
RTY6126	W303 MATa <i>ade2-1 ura3-1 his3-11,15 leu2-3-112 trp1-1 can1-100 cdc7-4</i>	2A, C, D	This study
RTY6153	W303 MATa <i>ade2-1 ura3-1 his3-11,15 leu2-3-112 trp1-1 can1-100 bob1-1</i>	2C, D	This study
RTY6154	W303 MATa <i>ade2-1 ura3-1 his3-11,15 leu2-3-112 trp1-1 can1-100 bob1-1 cdc7Δ::HIS3</i>	2C, D	This study
RTY6510	W303 MATa <i>ade2-1 ura3-1 his3-11,15 leu2-3-112 trp1-1 can1-100</i>	2D, 3B, 4A, C, 5A, B, F, 6B to E, G, 7B, C, 8A to C	This study
RTY6512	W303 MATa <i>ade2-1 ura3-1 his3-11,15 leu2-3-112 trp1-1 can1-100 cdc7-4</i>	2F, 4A, 4C to F, 5A to C, E to H, 6G, 7A to D, H to J, 8A to G, 9A to D, I	This study
RTY6513	W303 MATa <i>ade2-1 ura3-1 his3-11,15 leu2-3-112 trp1-1 can1-100 rif1d::NATMX</i>	2D, 3B, 5A, B, 6B to E, G	This study
RTY6514	W303 MATa <i>ade2-1 ura3-1 his3-11,15 leu2-3-112 trp1-1 can1-100 cdc7-4 rif1d::NATMX</i>	3A, 5A, B, 6G, 7A, D	This study
RTY6128	W303 MAT α <i>ade2-1 ura3-1 his3-11,15 leu2-3-112 trp1-1 can1-100 rif1d::NATMX</i>	3A	This study
RTY6130	W303 MAT α <i>ade2-1 ura3-1 his3-11,15 leu2-3-112 trp1-1 can1-100 cdc7-4 rif1d::NATMX</i>	3A	This study
YLH129-1	W303 MATa <i>ade2-1 ura3-1 his3-11,15 leu2-3-112 trp1-1 can1-100 cdc7-4 rif1d2-176-13MYC::HIS3MX6</i>	3A	36
YSM283	W303 MATa <i>ade2-1 ura3-1 his3-11,15 leu2-3-112 trp1-1 can1-100 cdc7-4 rif1-RVxF/SILK</i>	3A	36
W5094-1C	W303 MATa <i>ade2-1 ura3-1 his3-11,15 leu2-3-112 trp1-1 can1-100 ADE2 RAD5 RAD52-YFP</i>	3C	This study
ERY4824	W303 MATa <i>ade2-1 ura3-1 his3-11,15 leu2-3-112 trp1-1 can1-100 ADE2 RAD5 RAD52-YFP rif1d::URA3MX</i>	3C	This study
ASY4113	BY4743 MATa/ α <i>ura3Δ0/ura3Δ0 leu2Δ0/leu2Δ0 his3Δ1/his3Δ1 est2d::HPHMXMX/EST2</i>	3D, E	This study
ASY5059	BY4743 MATa/ α <i>ura3Δ0/ura3Δ0 leu2Δ0/leu2Δ0 his3Δ1/his3Δ1 est2d::HPHMXMX/EST2 rif1d::URA3MX/RIF1</i>	3D, E	This study
RTY6989	W303 MATa <i>ade2-1 ura3-1 his3-11,15 leu2-3-112 trp1-1 can1-100 sir2Δ::HPHMX</i>	4A, B	This study
RTY6991	W303 MATa <i>ade2-1 ura3-1 his3-11,15 leu2-3-112 trp1-1 can1-100 sir2Δ::HPHMX cdc7-4</i>	4A, B	This study
RTY6997	W303 MATa <i>ade2-1 ura3-1 his3-11,15 leu2-3-112 trp1-1 can1-100 hst1Δ::HPHMX</i>	4A, B	This study
RTY6998	W303 MATa <i>ade2-1 ura3-1 his3-11,15 leu2-3-112 trp1-1 can1-100 hst1Δ::HPHMX cdc7-4</i>	4A, B	This study
RTY6994	W303 MATa <i>ade2-1 ura3-1 his3-11,15 leu2-3-112 trp1-1 can1-100 hst2Δ::HPHMX</i>	4A	This study
RTY7001	W303 MATa <i>ade2-1 ura3-1 his3-11,15 leu2-3-112 trp1-1 can1-100 hst2Δ::HPHMX cdc7-4</i>	4A	This study
HMY210	W303 MATa <i>ade2-1 ura3-1 his3-11,15 leu2-3-112 trp1-1 can1-100 hst3Δ::HIS5+</i>	4C	From Alain Verreault's lab
RTY6383	W303 MAT α <i>ade2-1 ura3-1 his3-11,15 leu2-3-112 trp1-1 can1-100 cdc7-4 hst3Δ::HIS5+</i>	4C	This study
YMY6870	W303 MATa <i>ade2-1 ura3-1 his3-11,15 leu2-3-112 trp1-1 can1-100 hst4Δ::KANMX</i>	4C	This study
YMY6873	W303 MAT α <i>ade2-1 ura3-1 his3-11,15 leu2-3-112 trp1-1 can1-100 hst4Δ::KANMX cdc7-4</i>	4C	This study
RTY6511	W303 MATa <i>ade2-1 ura3-1 his3-11,15 leu2-3-112 trp1-1 can1-100 hst3Δ::HIS5+ hst4Δ::KANMX</i>	4C, 5A, B, F, 6B to E, G, 7B, C, 8A to C, 9A, E	This study
RTY6515	W303 MATa <i>ade2-1 ura3-1 his3-11,15 leu2-3-112 trp1-1 can1-100 hst3Δ::HIS5+ hst4Δ::KANMX cdc7-4</i>	4C, 5A to H, 6B to E, G, 7A to D, H to J, 8A to G, 9A to F, H, I	This study

(Continued)

TABLE 3 (Continued).

Strain name	Genotype	Figure	Reference
RTY6560	W303 MATa <i>ade2-1 ura3-1 his3-11,15 leu2-3-112 trp1-1 can1-100 cdc7-4 rtt109Δ::KANMX</i>	4D, 9A to D	This study
RTY6517	W303 MATa <i>ade2-1 ura3-1 his3-11,15 leu2-3-112 trp1-1 can1-100 hst3Δ::HIS5+ hst4Δ::KANMX cdc7-4 rif1Δ::NATMX</i>	5A, B, 6G, 7A	This study
RTY6694	W303 MATa <i>ade2-1 ura3-1 his3-11,15 leu2-3-112 trp1-1 can1-100 hst3Δ::HIS5+ hst4Δ::KANMX cdc7-4 [pCEN-HST3-URA3]</i>	5D	This study
ASY4249	BY4743 MATa <i>ura3Δ0 leu2Δ0 his3Δ1 hst3Δ::HPHMXMX hst4Δ::NATMX [pCEN-HST3::URA]</i>	6A	This study
ASY4900	BY4743 MATa <i>ura3Δ0 leu2Δ0 his3Δ1 hst3Δ::HPHMXMX hst4Δ::NATMX sir2Δ::KANMX rif1Δ::HIS3MX [pCEN-HST3::URA]</i>	6A	This study
ASY4903	BY4743 MATa <i>ura3Δ0 leu2Δ0 his3Δ1 hst3Δ::HPHMXMX hst4Δ::NATMX sir2Δ::KANMX [pCEN-HST3::URA]</i>	6A	This study
ASY4904	BY4743 MATa <i>ura3Δ0 leu2Δ0 his3Δ1 hst3Δ::HPHMXMX hst4Δ::NATMX rif1Δ::HIS3MX [pCEN-HST3::URA]</i>	6A	This study
RTY6700	W303 MATa <i>ade2-1 ura3-1 his3-11,15 leu2-3-112 trp1-1 can1-100 rtt109Δ::KANMX6</i>	6B, 9A, C	This study
RTY6461	BY4741 MATa <i>ura3Δ0 leu2Δ0 his3Δ1 met15Δ0 Rad52-GFP::HIS3MX</i>	6F	This study
RTY6463	BY4741 MATa <i>ura3Δ0 leu2Δ0 his3Δ1 met15Δ0 Rad52-GFP::HIS3MX rif1Δ::KANMX</i>	6F	This study
RTY6465	BY4741 MATa <i>ura3Δ0 leu2Δ0 his3Δ1 met15Δ0 Rad52-GFP::HIS3MX hst3Δ::HPHMXMX hst4Δ::NATMX</i>	6F	This study
RTY6467	BY4741 MATa <i>ura3Δ0 leu2Δ0 his3Δ1 met15Δ0 Rad52-GFP::HIS3MX hst3Δ::HPHMXMX hst4Δ::NATMX rif1Δ::KANMX</i>	6F	This study
HMY221	W303 MATa <i>ade2-1 ura3-1 his3-11,15 leu2-3-112 trp1-1 can1-100 hst3Δ::HIS5+ hst4Δ::KANMX</i>	6G, 7C	19
RTY6254	W303 MATa <i>ade2-1 ura3-1 his3-11,15 leu2-3-112 trp1-1 can1-100 hst3Δ::HIS5+ hst4Δ::KANMX rif1Δ::NATMX</i>	6G	This study
RTY6766	W303 MATa <i>ade2-1 ura3-52 his3-11 leu2-3-112 trp1Δ2 can1-100 p404-BrdU-inc::TRP/XbaI cdc7-4</i>	7E to G	This study
RTY6762	W303 MATa <i>ade2-1 ura3-52 his3-11 leu2-3-112 trp1Δ2 can1-100 p404-BrdU-inc::TRP/XbaI hst3Δ::HIS5+ hst4Δ::KANMX cdc7-4</i>	7E to G	This study
RTY6692	W303 MATa <i>ade2-1 ura3-1 his3-11,15 leu2-3-112 trp1-1 can1-100 rad9Δ::HPHMXMX hst3Δ::HIS5+ hst4Δ::KANMX</i>	8C	This study
RTY6667	W303 MATa <i>ade2-1 ura3-1 his3-11,15 leu2-3-112 trp1-1 can1-100 rad9Δ::HPHMX cdc7-4</i>	8C	This study
RTY6670	W303 MATa <i>ade2-1 ura3-1 his3-11,15 leu2-3-112 trp1-1 can1-100 rad9Δ::HPHMX cdc7-4 hst3Δ::HIS5+ hst4Δ::KANMX</i>	8C	This study
RTY6754	W303 MATa <i>ade2-1 ura3-1 his3-11,15 leu2-3-112 trp1-1 can1-100 cdc7-4 mrc1Δ::HIS5+ pRS405-mrc1aq::LEU2</i>	8D	This study

(Continued)

TABLE 3 (Continued).

Strain name	Genotype	Figure	Reference
RTY6752	W303 MATa <i>ade2-1 ura3-1 his3-11,15 leu2-3-112 trp1-1 can1-100 hst3Δ::HIS5+ hst4Δ::KANMX mrc1Δ::HIS5 + [pRS405-mrc1aq::LEU2]</i>	8D	This study
RTY6748	W303 MATa <i>ade2-1 ura3-1 his3-11,15 leu2-3-112 trp1-1 can1-100 cdc7-4 hst3Δ::HIS5+ hst4Δ::KANMX mrc1Δ::HIS5 + [pRS405-mrc1aq::LEU2]</i>	8D	This study
YMY6850	W303 MATa <i>ade2-1 ura3-1 his3-11,15 leu2-3-112 trp1-1 can1-100 cdc7-4 hst3Δ::HIS5+ hst4Δ::KANMX dbf4Δ::TRP1 his3::PDBF4-dbf4-4A::HIS3 sld3-38A-10his-13MYC::KANMX4</i>	8G	This study
RTY6778	W303 MATa <i>ade2-1 ura3-1 his3-11,15 leu2-3-112 trp1-1 can1-100 cdc7-4 dbf4Δ::TRP1 his3::PDBF4-dbf4 4A::HIS3 sld3-38A-10his-13MYC::KANMX4</i>	8G	This study
W303 WT	W303 MATα <i>ade2-1 ura3-52 his3-11,15 leu2-3-112 trp1-1 can1-100</i>	9A to C	NA
RTY6739	W303 MATa <i>ade2-1 ura3-1 his3-11,15 leu2-3-112 trp1-1 can1-100 hst3Δ::HIS5+ hst4Δ::KANMX cdc7-4 rtt109Δ::KANMX</i>	9A to D	This study
HMY133	W303 MATa <i>ade2-1 ura3-1 his3-11,15 leu2-3,112 trp1-1 can1-100 hht1-hhf1D::LEU2 hht2-hhf2D::kanMX3 [YCp22 HHT1 HHF1 TRP1]</i>	9E	This study
HMY135	W303 MATa <i>ade2-1 ura3-1 his3-11,15 leu2-3,112 trp1-1 can1-100 hht1-hhf1D::LEU2 hht2-hhf2D::kanMX3 [YCp22 hht1 K56Q HHF1 TRP1]</i>	9E	This study
YMY6894	W303 MATa <i>ade2-1 ura3-1 his3-11,15 leu2-3,112 trp1-1 can1-100 cdc7-4 hht1-hhf1D::LEU2 hht2-hhf2D::kanMX3 [YCp22 HHT1 HHF1 TRP1]</i>	9E	This study
YMY6895	W303 MATa <i>ade2-1 ura3-1 his3-11,15 leu2-3,112 trp1-1 can1-100 cdc7-4 hht1-hhf1D::LEU2 hht2-hhf2D::kanMX3 [YCp22 hht1 K56Q HHF1 TRP1]</i>	9E	This study
YMY6879	W303 MATa <i>ade2-1 ura3-1 his3-11,15 leu2-3-112 trp1-1 can1-100 hht1-hhf1Δ::LEU2 trp1::HHT1-HHF1::TRP1 hst3Δ::HIS5+ hst4Δ::KANMX cdc7-4</i>	9F, H	This study
YMY6878	W303 MATα <i>ade2-1 ura3-1 his3-11,15 leu2-3-112 trp1-1 can1-100 hht1-hhf1Δ::LEU2 trp1::HHT1 K56R-HHF1::TRP1 hst3Δ::HIS5+ hst4Δ::KANMX cdc7-4</i>	9F, H	This study
HMY152	W303 MATa <i>ade2-1 ura3-1 his3-11,15 leu2-3-112 trp1-1 can1-100 hht1-hhf1Δ::LEU2 hht2-hhf2Δ::KANMX3 trp1::HHT1-HHF1::TRP1</i>	9F	65
HMY140	W303 MATa <i>ade2-1 ura3-1 his3-11,15 leu2-3-112 trp1-1 can1-100 hht1-hhf1Δ::LEU2 hht2-hhf2Δ::KANMX3 trp1::HHT1 K56R-HHF1::TRP1</i>	9F	65
RTY6972	W303 MATa <i>ade2-1 ura3-1 his3-11, 15 leu2-3,112 trp1-1 can1-100 hht1-hhf1::LEU2 trp1::HHT1-HHF1::TRP1 cdc7-4</i>	9G	This study
RTY6981	W303 MATa <i>ade2-1 ura3-1 his3-11, 15 leu2-3,112 trp1-1 can1-100 hht1-hhf1::LEU2 trp1::HHT1 K56R-HHF1::TRP1 cdc7-4</i>	9G	This study

(Continued)

TABLE 3 (Continued).

Strain name	Genotype	Figure	Reference
RTY6974	W303 MATa <i>ade2-1 ura3-1 his3-11, 15 leu2-3,112 trp1-1 can1-100 hht1-hhf1::LEU2 trp1::HHT1-HHF1::TRP1 cdc7-4 hst3Δ::HIS5+ hst4Δ::KANMX</i>	9G	This study
RTY6979	W303 MATa <i>ade2-1 ura3-1 his3-11, 15 leu2-3,112 trp1-1 can1-100 hht1-hhf1::LEU2 trp1::HHT1 K56R-HHF1::TRP1 cdc7-4 hst3Δ::HIS5+ hst4Δ::KANMX</i>	9G	This study
YMY6865	W303 MATα <i>ade2-1 ura3-1 his3-11,15 leu2-3-112 trp1-1 can1-100 rtt101Δ::URA3MX cdc7-4</i>	9I	This study
YMY6861	W303 MATα <i>ade2-1 ura3-1 his3-11,15 leu2-3-112 trp1-1 can1-100 rtt101Δ::URA3MX hst3Δ::HIS5+ hst4Δ::KANMX cdc7-4</i>	9I	This study
YMY6874	W303 MATa <i>ade2-1 ura3-1 his3-11,15 leu2-3-112 trp1-1 can1-100 mms1Δ::URA3MX cdc7-4</i>	9I	This study
YMY6877	W303 MATa <i>ade2-1 ura3-1 his3-11,15 leu2-3-112 trp1-1 can1-100 mms1Δ::URA3MX hst3Δ::HIS5+ hst4Δ::KANMX cdc7-4</i>	9I	This study

containing 50 μg/mL uracil 0.1% of 5-fluoroorotic acid (Bioshop) (5-FoA). Plates were incubated at the indicated temperature for 48–72 h.

Cell cycle analysis by flow cytometry. DNA content/cell cycle analysis by flow cytometry was performed as previously described.⁷⁷ Flow cytometry was performed using a BD Biosciences FACS Calibur instrument equipped with CellQuest software. Data were analyzed using FlowJo 10.8.1 (FlowJo, LLC). Cell cycle analyses were performed using Watson model; G1 and G2 peaks were constrained based on asynchronous population for each strain.

Immunoblotting. Four OD of cells were pelleted and frozen at –80 °C prior whole-cell extraction. Cells were extracted using 0.1 M NaOH for 5 min at room temperature as described before,⁷⁸ or using standard trichloroacetic acid (TCA) and glass beads method.⁷⁹ Protein extracts were quantified using bicinchoninic acid (BCA) protein assay kit according to the manufacturer's protocol (Pierce). SDS-PAGE and transfer were performed using standard methods. Anti-H3 (Abcam; cat: ab1791) and anti-Rad53 (Abcam; cat: ab104232) were purchased from Abcam. Anti-Mcm4 (sc-166036) was purchased from Santa-Cruz. Anti-H3 K56ac (AV105) and anti-H2A-S129-P (AV137) antibodies were generously provided by Dr Alain Verreault (Université de Montréal, Canada). Goat anti-rabbit (BioRad; cat: 1705046), goat anti-mouse (Bio Rad; cat: 1705047) and goat anti-rat (Abcam; cat: ab97057) were used as secondary antibodies. Protein visualization was realized by chemiluminescence using Pierce ECL Western Blotting Substrate. Images were captured using an Azure c600 chemiluminescence Imaging System.

Isolation of phosphoproteins. Proteins from 25 OD of cells were extracted using standard TCA and glass beads method. Protein pellets were resuspended in 100 μL of urea 8 μM. Samples were then diluted 10-fold before protein quantification by BCA protein assay (Pierce). One milligram of protein was used for phosphoprotein isolation using Pro-Q Diamond Phosphoprotein Enrichment Kit according to the manufacturer's protocol (ThermoFisher; cat: P33358). Immunoblotting was performed on the input and eluate to quantify phosphorylated proteins.

Fluorescence microscopy. Cells were fixed in 0.1 M of potassium phosphate buffer pH 6.4 containing 3.7% formaldehyde (Sigma-Aldrich) and slides were prepared as described before.⁶⁰ Images were taken by fluorescence microscopy using a 60× objective numerical aperture (NA, 1.42) on DeltaVision instrument (GE Healthcare). Image analysis was performed using SoftWoRx 7 software and FIJI 1.53.

Pulse-field gel electrophoresis (PFGE). Yeast chromosome migration by PFGE has been performed as described previously.⁵¹ Briefly, 2.5 OD of cells were washed in 50 mM EDTA, then resuspended in 55 °C-heated 0.25 mg/mL Zymolyase 100 T solution containing 1% low melting point agarose (LMPA). The mixture is poured into the plug former and placed at 4 °C to set. Plugs were then incubated in 0.5 M EDTA, 100 mM TRIS-HCl supplemented with 500 μL of β-mercaptoethanol at 37 °C overnight followed by two quick washes in 50 mM EDTA. Subsequently, plugs were incubated in 0.325 M EDTA, 1% N-Lauroylsarcosine, 15 mg proteinase K and 1 mg RNase overnight at 37 °C. Plugs were washed in 1× TE buffer at 4 °C for 1 h. One percent agarose gel was prepared in 0.5× TBE buffer. When ready to run, plugs were inserted into the gel. The run is performed at pump setting 70 and at 14 °C. First, gel was kept with these parameters for 1 h to equilibrate. Migration was performed at 6 V/cm with an angle of 120°. Switch time between pulses were 60 s for the first 15 h, then 90 s for the remaining 9 h. After the migration, gel was stained in H₂O + 100 μL SYBR Green (Life technologies; cat: S7563) for 1 h. Images were captured using an Azure c600 chemiluminescence Imaging System.

TABLE 4 PCR primers used in this study

Primer name	Sequence (5'–3')	Figure
ARS305_probe_F	ATCGTGTAAGCTGGGGTGAC	5C
ARS305_probe_R	AGTGGCGTTAGGTTCAATGC	5C
ARS305_qPCR-2_F	TACTTTGTAGTTCTTAAAGC	5D
ARS305_qPCR-2_R	CTTTAATGAGTATTTGATCC	5D
ARS315_qPCR_F	TTCTTCGCGCTCAACTTTC	5E, G
ARS315_qPCR_R	TTTCTTGGCGCTACGATGTG	5E, G
ARS1211_qPCR-2_F	TCCACTGCGTTTTATGTATC	5F
ARS1211_qPCR-2_R	TCAGTTGGGCTTTGTTTAAAG	5F
ARS305_qPCR_F	TACACGGGGGCTAAAAACGG	5G, H
ARS305_qPCR_R	GCACTTTGATGAGGTCTCTAGC	5G, H
ARS1211_qPCR_F	TTGGGCTAGGAGAAAAGTGGC	5G, H
ARS1211_qPCR_R	CGAACGCAATGTGCCAAGAA	5G, H
ARS300-F	TCACCCATCTCTACCATCA	5G
ARS300-R	GATGGGCGTTATGCGTAAAT	5G
NegV_qPCR_F	TAATTGCTGAGCGTTGCATGTT	5G, H
NegV_qPCR_R	GCCTCTACAGTACCGTGGGGAGA	5G, H
ARS607_qPCR_F	GGCTCGTGCATTAAGCTTGT	5H
ARS607_qPCR_R	CACGCCAAACATTGCATTTA	5H

Alkaline gel electrophoresis and Southern blotting. Samples were denatured by heating at 70 °C in loading buffer (30 mM NaOH, 1 mM EDTA, 3% Ficoll 400, 0.01% bromocresol green). Denatured DNA was run in a 1% agarose gel in alkaline electrophoresis buffer (30 mM NaOH, 2 mM EDTA) at 3 V/cm. Southern blotting was performed using a digoxigenin (DIG)-labeled probe as described before.⁸⁰ The ARS305 probe was generated by PCR using primers ARS305_probe_F and ARS305_probe_R (Table 4) and the PCR DIG Labeling Mix (Roche). Membranes were imaged using an Azure c600 chemiluminescence Imaging System.

Measurement of BrdU incorporation by DNA immunoprecipitation and qPCR. Measurement of BrdU signal was performed as described previously.⁸¹ Briefly, 400 µg/mL BrdU (BioShop; cat: BRU222.5) was added to cells released toward S phase at 37 °C for 1 h. Ten OD of cells were harvested per condition. Cells were immediately fixed in 70% ethanol. DNA was extracted as described before,⁸² then sonicated at 25% for four cycles of 15 s. DNA samples were then purified using EZ-10 Spin Column PCR Products Purification Kit (Bio Basics) according to the manufacturer's instructions. DNA was quantified using a fluorometer (Turner Biosystems) according to the manufacturer's protocol. Five hundred nanograms of genomic DNA was used per condition for immunoprecipitation. DNA samples were mixed with 0.1 µg/µL of blocking DNA and denatured at 95 °C for 10 min followed by snap-cooling on ice for 5 min. Then, DNA samples were incubated with anti-BrdU antibody (Invitrogen; cat: ZBU30) antibody in 1 × PBS + 0.0625% Triton X-100 at 4 °C for 4 h. 15 µL of washed Protein G MagBeads (GenScript; cat: L00274) were added to the DNA samples and incubated overnight at 4 °C. Immunoprecipitated DNA samples were washed three times with 500 µL 1 × PBS + 0.0625% Triton X-100 and twice with 1 × TE pH 7.6. Then, samples were eluted with TE pH 7.6 1% sodium dodecyl sulfate (SDS) at 65 °C for 15 min. The eluate is then purified using EZ-10 Spin Column PCR Products Purification Kit (Bio Basics) according to manufacturer's instructions. Three microliters of immunoprecipitated sample or 0.5 ng of input sample was used per qPCR reaction (qPCR Master Mix, APEXBio; cat: K1070). PCR was performed using an Applied Biosystems 7500 instrument (software version 2.3). PCR primers are listed in Table 4. BrdU incorporation quantification was performed using the standard percent of the input method. To normalize for eventual differences in BrdU incorporation capacity between strains, IP/input value was divided by the IP/input value obtained using the same strain which was synchronized in G1 and then released in S phase for 1 h in presence of 200 mM HU at 25 °C.

Measurement of DNA content by quantitative PCR. Genomic DNA from 1 OD₆₃₀ of cells was extracted and purified as previously described.⁸² 3 ng of DNA was used per qPCR reaction (qPCR Master Mix, NEB). PCR was performed using an Applied Biosystems 7500 instrument (software version 2.3). PCR primers are listed in Table 4. Briefly, qPCR signal for a given origin was first normalized to the signal obtained from the NegV locus (ChrV: 532538-532516).⁶⁹ This region is located ≈12 kb from ARS521, an origin which has not been detected to be active in several studies according to OriDB (<http://cerevisiae.oridb.org/>) and ≈18 kb from ARS522, a subtelomeric origin of replication activated in late S. As such, the NegV locus is expected to be replicated in late S, and therefore to generally remain unreplicated in a majority of *cdc7-4* and *cdc7-4 hst3Δ hst4Δ* cells 30 min post-release from G1 arrest toward S phase. The NegV-normalized S phase signal was divided by the NegV-normalized signal obtained from alpha factor arrested (G1) cells. Complete replication of an origin is therefore expected to result in a ratio of S phase over G1 signal of 2.

Statistical analysis. Data are represented as mean \pm standard error of the mean (SEM) unless otherwise specified. All analyses were performed using GraphPad Prism 8. Statistical tests are described in figure legends.

ACKNOWLEDGMENTS

H.W. is the recipient of a Chercheur-boursier Sénior scholarship from Fonds de la Recherche du Québec-Santé (award #281795; <https://frq.gouv.qc.ca>). This work was supported by Natural Sciences and Engineering Research Council of Canada (NSERC; <https://www.nserc-crsng.gc.ca>) Discovery Grants to H.W. (RGPIN-2019-05082) and E. B. A. (RGPIN-2021-04110), a NSERC Discovery Accelerator Supplement to H.W. (RGPAS-2019-00009), and by a Fonds de la Recherche du Québec-Nature et Technologies grant (2018-PR-206098; <https://frq.gouv.qc.ca>) to H.W. C.N. is supported by the Canadian Foundation for Innovation (CFI; <https://www.innovation.ca/>) and is a Canada Research Chairs (CRC; <https://www.chairs-chaire.gc.ca/>) Tier 1 Chair. O.A. is the recipient of a doctoral scholarship from Fonds de la Recherche du Québec-Santé. The funders had no role in study design, data collection and analysis, decision to publish, or preparation of the manuscript. We thank Dr David Shore (Université de Genève) for providing yeast strains, Dr Alain Verreault (Université de Montréal) for providing yeast strains, anti-H3 K56ac and anti-H2A S129-P antibodies, and Dr Elliot A. Drobetsky (Université de Montréal) for critical reading of the manuscript.

ORCID

Hugo Wurtele  <http://orcid.org/0000-0002-5733-1711>

DATA AVAILABILITY STATEMENT

Data available within the article or its supplementary materials, and at <https://doi.org/10.5683/SP3/MPVRT7>.

DISCLOSURE STATEMENT

No potential conflict of interest was reported by the author(s).

REFERENCES

- Remus D, Diffley JF. Eukaryotic DNA replication control: lock and load, then fire. *Curr Opin Cell Biol.* 2009;21:771–777. doi:10.1016/j.ceb.2009.08.002.
- Tanaka T, Umemori T, Endo S, Muramatsu S, Kanemaki M, Kamimura Y, Obuse C, Araki H. Sld7, an Sld3-associated protein required for efficient chromosomal DNA replication in budding yeast. *EMBO J.* 2011;30:2019–2030. doi:10.1038/emboj.2011.115.
- Mantiero D, Mackenzie A, Donaldson A, Zegerman P. Limiting replication initiation factors execute the temporal programme of origin firing in budding yeast. *EMBO J.* 2011;30:4805–4814. doi:10.1038/emboj.2011.404.
- Branzei D, Foiani M. The checkpoint response to replication stress. *DNA Repair (Amst).* 2009;8:1038–1046.
- Bacal J, Moriel-Carretero M, Pardo B, Barthe A, Sharma S, Chabes A, Lengronne A, Pasero P. Mrc1 and Rad9 cooperate to regulate initiation and elongation of DNA replication in response to DNA damage. *EMBO J.* 2018;37:e99319. doi:10.15252/emboj.201899319.
- Santocanale C, Diffley JF. A Mec1- and Rad53-dependent checkpoint controls late-firing origins of DNA replication. *Nature.* 1998;395:615–618. doi:10.1038/27001.
- Zegerman P, Diffley JFX. Checkpoint-dependent inhibition of DNA replication initiation by Sld3 and Dbf4 phosphorylation. *Nature.* 2010;467:474–478. doi:10.1038/nature09373.
- Toledo LI, Altmeyer M, Rask M-B, Lukas C, Larsen DH, Povlsen LK, Bekker-Jensen S, Mailand N, Bartek J, Lukas J. ATR prohibits replication catastrophe by preventing global exhaustion of RPA. *Cell.* 2013;155:1088–1103. doi:10.1016/j.cell.2013.10.043.
- Smith OK, Aladjem MI. Chromatin structure and replication origins: determinants of chromosome replication and nuclear organization. *J Mol Biol.* 2014;426:3330–3341. doi:10.1016/j.jmb.2014.05.027.
- Méchali M, Yoshida K, Coulombe P, Pasero P. Genetic and epigenetic determinants of DNA replication origins, position and activation. *Curr Opin Genet Dev.* 2013;23:124–131. doi:10.1016/j.gde.2013.02.010.
- Yoshida K, Bacal J, Desmarais D, Padiouleau I, Tsaponina O, Chabes A, Pantescio V, Dubois E, Parrinello H, Skrzypczak M, et al. The histone deacetylases sir2 and rpd3 act on ribosomal DNA to control the replication program in budding yeast. *Mol Cell.* 2014;54:691–697. doi:10.1016/j.molcel.2014.04.032.
- Brachmann CB, Sherman JM, Devine SE, Cameron EE, Pillus L, Boeke JD. The SIR2 gene family, conserved from bacteria to humans, functions in silencing, cell cycle progression, and chromosome stability. *Genes Dev.* 1995;9:2888–2902. doi:10.1101/gad.9.23.2888.
- Pasero P, Bensimon A, Schwob E. Single-molecule analysis reveals clustering and epigenetic regulation of replication origins at the yeast rDNA locus. *Genes Dev.* 2002;16:2479–2484. doi:10.1101/gad.232902.
- Stevenson JB, Gottschling DE. Telomeric chromatin modulates replication timing near chromosome ends. *Genes Dev.* 1999;13:146–151. doi:10.1101/gad.13.2.146.
- Irlbacher H, Franke J, Manke T, Vingron M, Ehrenhofer-Murray AE. Control of replication initiation and heterochromatin formation in *Saccharomyces cerevisiae* by a regulator of meiotic gene expression. *Genes Dev.* 2005;19:1811–1822. doi:10.1101/gad.334805.
- Weber JM, Irlbacher H, Ehrenhofer-Murray AE. Control of replication initiation by the Sum1/Rfm1/Hst1 histone deacetylase. *BMC Mol Biol.* 2008;9:100. doi:10.1186/1471-2199-9-100.
- Cockell MM, Perrod S, Gasser SM. Analysis of Sir2p domains required for rDNA and telomeric silencing in *Saccharomyces cerevisiae*. *Genetics.* 2000;154:1069–1083. doi:10.1093/genetics/154.3.1069.
- Lamming DW, Latorre-Esteves M, Medvedik O, Wong SN, Tsang FA, Wang C, Lin S-J, Sinclair DA. HST2 mediates SIR2-independent life-span

- extension by calorie restriction. *Science*. 2005;309:1861–1864. doi:10.1126/science.1113611.
19. Celic I, Masumoto H, Griffith WP, Meluh P, Cotter RJ, Boeke JD, Verreault A. The sirtuins hst3 and Hst4p preserve genome integrity by controlling histone h3 lysine 56 deacetylation. *Curr Biol*. 2006;16:1280–1289. doi:10.1016/j.cub.2006.06.023.
 20. Fillingham J, Recht J, Silva AC, Suter B, Emili A, Stagljar I, Krogan NJ, Allis CD, Keogh M-C, Greenblatt JF. Chaperone control of the activity and specificity of the histone H3 acetyltransferase Rtt109. *Mol Cell Biol*. 2008;28:4342–4353. doi:10.1128/MCB.00182-08.
 21. Driscoll R, Hudson A, Jackson SP. Yeast Rtt109 promotes genome stability by acetylating histone H3 on lysine 56. *Science*. 2007;315:649–652. doi:10.1126/science.1135862.
 22. Maas NL, Miller KM, DeFazio LG, Toczyski DP. Cell cycle and checkpoint regulation of histone H3 K56 acetylation by Hst3 and Hst4. *Mol Cell*. 2006;23:109–119. doi:10.1016/j.molcel.2006.06.006.
 23. Celic I, Verreault A, Boeke JD. Histone H3 K56 hyperacetylation perturbs replisomes and causes DNA damage. *Genetics*. 2008;179:1769–1784. doi:10.1534/genetics.108.088914.
 24. Simoneau A, Delgosaie N, Celic I, Dai J, Abshiru N, Costantino S, Thibault P, Boeke JD, Verreault A, Wurtele H. Interplay between histone H3 lysine 56 deacetylation and chromatin modifiers in response to DNA damage. *Genetics*. 2015;200:185–205. doi:10.1534/genetics.115.175919.
 25. Sauve AA, Wolberger C, Schramm VL, Boeke JD. The biochemistry of sirtuins. *Annu Rev Biochem*. 2006;75:435–465. doi:10.1146/annurev.biochem.74.082803.133500.
 26. Simoneau A, Ricard É, Weber S, Hammond-Martel I, Wong LH, Sellam A, Giaever G, Nislow C, Raymond M, Wurtele H. Chromosome-wide histone deacetylation by sirtuins prevents hyperactivation of DNA damage-induced signaling upon replicative stress. *Nucleic Acids Res*. 2016;44:2706–2726. doi:10.1093/nar/gkv1537.
 27. Simoneau A, Ricard É, Wurtele H. An interplay between multiple sirtuins promotes completion of DNA replication in cells with short telomeres. *PLoS Genet*. 2018;14:e1007356. doi:10.1371/journal.pgen.1007356.
 28. Irene C, Theis JF, Gresham D, Soteropoulos P, Newlon CS. Hst3p, a histone deacetylase, promotes maintenance of *Saccharomyces cerevisiae* chromosome III lacking efficient replication origins. *Mol Genet Genomics*. 2016;291:271–283. doi:10.1007/s00438-015-1105-8.
 29. Barazandeh M, Kriti D, Nislow C, Giaever G. The cellular response to drug perturbation is limited: comparison of large-scale chemogenomic fitness signatures. *BMC Genomics*. 2022;23:197. doi:10.1186/s12864-022-08395-x.
 30. John FD. Regulation of early events in chromosome replication. *Curr Biol*. 2004;14:R778–R786. doi:10.1016/j.cub.2004.09.019.
 31. Hardy CF, Dryga O, Seematter S, Pahl PM, Sclafani RA. mcm5/cdc46-bob1 bypasses the requirement for the S phase activator Cdc7p. *Proc Natl Acad Sci USA*. 1997;94:3151–3155. doi:10.1073/pnas.94.7.3151.
 32. Hiraga S-I, Alvino GM, Chang F, Lian H-Y, Sridhar A, Kubota T, Brewer BJ, Weinreich M, Raghuraman MK, Donaldson AD. Rif1 controls DNA replication by directing protein phosphatase 1 to reverse Cdc7-mediated phosphorylation of the MCM complex. *Genes Dev*. 2014;28:372–383. doi:10.1101/gad.231258.113.
 33. Mattarocci S, Shyian M, Lemmens L, Damay P, Altintas DM, Shi T, Bartholomew CR, Thomä NH, Hardy CFJ, Shore D. Rif1 controls DNA replication timing in yeast through the PP1 phosphatase Glc7. *Cell Rep*. 2014;7:62–69. doi:10.1016/j.celrep.2014.03.010.
 34. Hayano M, Kanoh Y, Matsumoto S, Renard-Guillet C, Shirahige K, Masai H. Rif1 is a global regulator of timing of replication origin firing in fission yeast. *Genes Dev*. 2012;26:137–150. doi:10.1101/gad.178491.111.
 35. Davé A, Cooley C, Garg M, Bianchi A. Protein phosphatase 1 recruitment by Rif1 regulates DNA replication origin firing by counteracting DDK activity. *Cell Rep*. 2014;7:53–61. doi:10.1016/j.celrep.2014.02.019.
 36. Hafner L, Lezaja A, Zhang X, Lemmens L, Shyian M, Albert B, Follonier C, Nunes JM, Lopes M, Shore D, et al. Rif1 binding and control of chromosome-internal DNA replication origins is limited by telomere sequestration. *Cell Rep*. 2018;23:983–992. doi:10.1016/j.celrep.2018.03.113.
 37. Stead BE, Brandl CJ, Davey MJ. Phosphorylation of Mcm2 modulates Mcm2-7 activity and affects the cell's response to DNA damage. *Nucleic Acids Res*. 2011;39:6998–7008. doi:10.1093/nar/gkr371.
 38. Stead BE, Brandl CJ, Sandre MK, Davey MJ. Mcm2 phosphorylation and the response to replicative stress. *BMC Genet*. 2012;13:36. doi:10.1186/1471-2156-13-36.
 39. Downs JA, Lowndes NF, Jackson SP. A role for *Saccharomyces cerevisiae* histone H2A in DNA repair. *Nature*. 2000;408:1001–1004. doi:10.1038/35050000.
 40. Lisby M, Rothstein R, Mortensen UH. Rad52 forms DNA repair and recombination centers during S phase. *Proc Natl Acad Sci USA*. 2001;98:8276–8282. doi:10.1073/pnas.121006298.
 41. Marcand S, Gilson E, Shore D. A protein-counting mechanism for telomere length regulation in yeast. *Science*. 1997;275:986–990. doi:10.1126/science.275.5302.986.
 42. Han J, Zhou H, Horazzdovsky B, Zhang K, Xu R-M, Zhang Z. Rtt109 acetylates histone H3 lysine 56 and functions in DNA replication. *Science*. 2007;315:653–655. doi:10.1126/science.1133234.
 43. Thamy S, Newcomb B, Kim J, Gatbonton T, Foss E, Simon J, Bedalov A. Hst3 is regulated by Mec1-dependent proteolysis and controls the S phase checkpoint and sister chromatid cohesion by deacetylating histone H3 at lysine 56. *J Biol Chem*. 2007;282:37805–37814. doi:10.1074/jbc.M706384200.
 44. Mishra PK, Wood H, Stanton J, Au W-C, Eisenstatt JR, Boeckmann L, Sclafani RA, Weinreich M, Bloom KS, Thorpe PH, et al. Cdc7-mediated phosphorylation of Cse4 regulates high-fidelity chromosome segregation in budding yeast. *Mol Biol Cell*. 2021;32:ar15. doi:10.1091/mbc.E21-06-0323.
 45. Seoane AI, Morgan DO. Firing of replication origins frees Dbf4-Cdc7 to target *eco1* for destruction. *Curr Biol*. 2017;27:2849–2855.e2. doi:10.1016/j.cub.2017.07.070.
 46. Díaz-Martínez LA, Clarke DJ. Chromosome cohesion and the spindle checkpoint. *Cycl Cell*. 2009;8:2733–2740. doi:10.4161/cc.8.17.9403.
 47. Alvaro D, Lisby M, Rothstein R. Genome-wide analysis of Rad52 foci reveals diverse mechanisms impacting recombination. *PLoS Genet*. 2007;3:e228. doi:10.1371/journal.pgen.0030228.
 48. Muñoz-Galván S, Jimeno S, Rothstein R, Aguilera A. Histone H3K56 acetylation, Rad52, and non-DNA repair factors control double-strand break repair choice with the sister chromatid. *PLoS Genet*. 2013;9:e1003237. doi:10.1371/journal.pgen.1003237.
 49. Hiraga S-I, Monerawela C, Katou Y, Shaw S, Clark KR, Shirahige K, Donaldson AD. Budding yeast Rif1 binds to replication origins and protects DNA at blocked replication forks. *EMBO Rep*. 2018;19:e46222. doi:10.15252/embr.201846222.
 50. Jenkinson F, Tan KW, Schöpf B, Santos MM, Zegerman P. Dephosphorylation of the pre-initiation complex is critical for origin firing. *Mol Cell*. 2023;83:12–25.e10. doi:10.1016/j.molcel.2022.12.001.
 51. Maringele L, Lydall D. Pulsed-field gel electrophoresis of budding yeast chromosomes. *Methods Mol Biol*. 2006;313:65–73. doi:10.1385/1-59259-958-3:065.
 52. Yekezare M, Gómez-González B, Diffley JFX. Controlling DNA replication origins in response to DNA damage—inhibit globally, activate locally. *J Cell Sci*. 2013;126:1297–1306. doi:10.1242/jcs.096701.
 53. Zhao X, Chabes A, Domkin V, Thelander L, Rothstein R. The ribonucleotide reductase inhibitor Sml1 is a new target of the Mec1/Rad53 kinase cascade during growth and in response to DNA damage. *EMBO J*. 2001;20:3544–3553. doi:10.1093/emboj/20.13.3544.
 54. Osborn AJ, Elledge SJ. Mrc1 is a replication fork component whose phosphorylation in response to DNA replication stress activates Rad53. *Genes Dev*. 2003;17:1755–1767. doi:10.1101/gad.1098303.
 55. Hall-Jackson CA, Cross DA, Morrice N, Smythe C. ATR is a caffeine-sensitive, DNA-activated protein kinase with a substrate specificity distinct from DNA-PK. *Oncogene*. 1999;18:6707–6713. doi:10.1038/sj.onc.1203077.
 56. Osman F, McCready S. Differential effects of caffeine on DNA damage and replication cell cycle checkpoints in the fission yeast *Schizosaccharomyces pombe*. *Mol Gen Genet*. 1998;260:319–334. doi:10.1007/s004380050901.
 57. Abshiru N, Ippersiel K, Tang Y, Yuan H, Marmorstein R, Verreault A, Thibault P. Chaperone-mediated acetylation of histones by Rtt109 identified by quantitative proteomics. *J Proteomics*. 2013;81:80–90. doi:10.1016/j.jprot.2012.09.026.
 58. Tang Y, Holbert MA, Delgosaie N, Wurtele H, Guillemette B, Meeth K, Yuan H, Drogaris P, Lee E-H, Durette C, et al. Structure of the Rtt109-AcCoA/Vps75 complex and implications for chaperone-mediated histone acetylation. *Structure*. 2011;19:221–231. doi:10.1016/j.str.2010.12.012.
 59. Collins SR, Miller KM, Maas NL, Roguev A, Fillingham J, Chu CS, Schuldiner M, Gebbia M, Recht J, Shales M, et al. Functional dissection of protein complexes involved in yeast chromosome biology using a genetic interaction map. *Nature*. 2007;446:806–810. doi:10.1038/nature05649.
 60. Wurtele H, Kaiser GS, Bacal J, St-Hilaire E, Lee E-H, Tsao S, Dorn J, Maddox P, Lisby M, Pasero P, et al. Histone h3 lysine 56 acetylation and the response to DNA replication fork damage. *Mol Cell Biol*. 2012;32:154–172. doi:10.1128/MCB.05415-11.

61. Han J, Zhang H, Zhang H, Wang Z, Zhou H, Zhang Z. A Cul4 E3 ubiquitin ligase regulates histone hand-off during nucleosome assembly. *Cell*. 2013;155:817–829. doi:10.1016/j.cell.2013.10.014.
62. Roberts TM, Zaidi IW, Vaisica JA, Peter M, Brown GW. Regulation of Rtt107 recruitment to stalled DNA replication forks by the cullin Rtt101 and the Rtt109 acetyltransferase. *Mol Biol Cell*. 2008;19:171–180. doi:10.1091/mbc.E07-09-0961.
63. Li Q, Zhou H, Wurtele H, Davies B, Horazdovsky B, Verreault A, Zhang Z. Acetylation of histone H3 lysine 56 regulates replication-coupled nucleosome assembly. *Cell*. 2008;134:244–255. doi:10.1016/j.cell.2008.06.018.
64. Hammond-Martel I, Verreault A, Wurtele H. Chromatin dynamics and DNA replication roadblocks. *DNA Repair (Amst)*. 2021;104:103140. doi:10.1016/j.dnarep.2021.103140.
65. Masumoto H, Hawke D, Kobayashi R, Verreault A. A role for cell-cycle-regulated histone H3 lysine 56 acetylation in the DNA damage response. *Nature*. 2005;436:294–298. doi:10.1038/nature03714.
66. Huisinga KL, Pugh BF. A genome-wide housekeeping role for TFIIID and a highly regulated stress-related role for SAGA in *Saccharomyces cerevisiae*. *Mol Cell*. 2004;13:573–585. doi:10.1016/s1097-2765(04)00087-5.
67. Theis JF, Irene C, Dershowitz A, Brost RL, Tobin ML, di Sanzo FM, Wang J-Y, Boone C, Newlon CS. The DNA damage response pathway contributes to the stability of chromosome III derivatives lacking efficient replicators. *PLoS Genet*. 2010;6:e1001227. doi:10.1371/journal.pgen.1001227.
68. Davidson MB, Katou Y, Keszthelyi A, Sing TL, Xia T, Ou J, Vaisica JA, Thevakumaran N, Marjavaara L, Myers CL, et al. Endogenous DNA replication stress results in expansion of dNTP pools and a mutator phenotype. *EMBO J*. 2012;31:895–907. doi:10.1038/emboj.2011.485.
69. Gershon L, Kupiec M. A novel role for Dun1 in the regulation of origin firing upon hyper-acetylation of H3K56. *PLoS Genet*. 2021;17:e1009391. doi:10.1371/journal.pgen.1009391.
70. Mimura S, Yamaguchi T, Ishii S, Noro E, Katsura T, Obuse C, Kamura T. Cul8/Rtt101 forms a variety of protein complexes that regulate DNA damage response and transcriptional silencing. *J Biol Chem*. 2010;285:9858–9867. doi:10.1074/jbc.M109.082107.
71. Ericson E, Hoon S, St Onge RP, Giaever G, Nislow C. Exploring gene function and drug action using chemogenomic dosage assays. *Methods Enzymol*. 2010;470:233–255. doi:10.1016/S0076-6879(10)70010-0.
72. Smith AM, Durbic T, Oh J, Urbanus M, Proctor M, Heisler LE, Giaever G, Nislow C. Competitive genomic screens of barcoded yeast libraries. *J Vis Exp*. 2011;54:2864. doi:10.3791/2864.
73. Pierce SE, Davis RW, Nislow C, Giaever G. Genome-wide analysis of bar-coded *Saccharomyces cerevisiae* gene-deletion mutants in pooled cultures. *Nat Protoc*. 2007;2:2958–2974. doi:10.1038/nprot.2007.427.
74. Boyle EI, Weng S, Gollub J, Jin H, Botstein D, Cherry JM, Sherlock G. GO::TermFinder—open source software for accessing Gene Ontology information and finding significantly enriched Gene Ontology terms associated with a list of genes. *Bioinformatics*. 2004;20:3710–3715. doi:10.1093/bioinformatics/bth456.
75. Cherry JM, Hong EL, Amundsen C, Balakrishnan R, Binkley G, Chan ET, Christie KR, Costanzo MC, Dwight SS, Engel SR, et al. Saccharomyces Genome Database: the genomics resource of budding yeast. *Nucleic Acids Res*. 2012;40:D700–D705. doi:10.1093/nar/gkr1029.
76. Supek F, Bošnjak M, Škunca N, Šmuc T. REVIGO summarizes and visualizes long lists of Gene Ontology terms. *PLoS One*. 2011;6:e21800. doi:10.1371/journal.pone.0021800.
77. Haase SB, Reed SI. Improved flow cytometric analysis of the budding yeast cell cycle. *Cell Cycle*. 2002;1:117–121. doi:10.4161/cc.1.2.114.
78. Kushnirov VV. Rapid and reliable protein extraction from yeast. *Yeast*. 2000;16:857–860. doi:10.1002/1097-0061(20000630)16:9<857::AID-YEA561>3.0.CO;2-B.
79. Grallert A, Hagan IM. Preparation of protein extracts from *Schizosaccharomyces pombe* using trichloroacetic acid precipitation. *Cold Spring Harb Protoc*. 2017;2017:pdb.prot091579. doi:10.1101/pdb.prot091579.
80. Viterbo D, Marchal A, Mosbach V, Poggi L, Vaysse-Zinkhöfer W, Richard G-F. A fast, sensitive and cost-effective method for nucleic acid detection using non-radioactive probes. *Biol Methods Protoc*. 2018;3:bpy006. doi:10.1093/biomethods/bpy006.
81. Viggiani CJ, Knott SRV, Aparicio OM. Genome-wide analysis of DNA synthesis by BrdU immunoprecipitation on tiling microarrays (BrdU-IP-Chip) in *Saccharomyces Cerevisiae*. *Cold Spring Harb Protoc*. 2010;2010:pdb.prot5385. doi:10.1101/pdb.prot5385.
82. Dymond JS. Preparation of genomic DNA from *Saccharomyces cerevisiae*. *Methods Enzymol*. 2013;529:153–160. doi:10.1016/B978-0-12-418687-3.00012-4.